



fiducial reference  
temperature  
measurements



**esa**

## Fiducial Reference Measurements for validation of Surface Temperature from Satellites (FRM4STS)

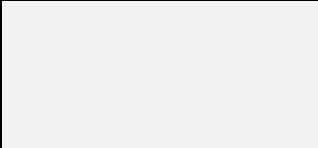
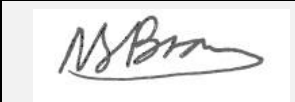
ESA Contract No. 4000113848\_15I-LG

# D100 - Technical Report 2: Results from the 4<sup>th</sup> CEOS TIR FRM Field Radiometer Laboratory Inter-comparison Exercise

## Part 3 of 4: Water surface temperature comparison of radiation thermometers

JUNE 2017

Reference	OFE-D100(Part 4)-V1-Iss-1=Ver-1-Draft
Issue	1
Revision	1
Date of Issue	23 June 2017
Document Type	TR-2

Approval/Acceptance			
<b>ESA</b> Craig Donlon Technical Officer		<b>NPL</b> Andrew Brown Project Manager	 Andrew Brown, NPL
	<i>Signature</i>		<i>Signature</i>

**2016 comparison of IR brightness temperature measurements in support of satellite validation. Part 3: Water surface temperature comparison of radiation thermometers.**

**I. Barker Snook, E. Theocharous and N. P. Fox**

June 2017



## 2016 comparison of IR brightness temperature measurements in support of satellite validation. Part 3: Water surface temperature comparison of radiation thermometers.

I. Barker Snook, E. Theocharous and N. P. Fox  
Environmental Division

### Abstract

Under the auspices of CEOS, a comparison of terrestrial based infrared (IR) radiometric instrumentation used to support calibration and validation of satellite borne sensors with emphasis on sea/water/land surface temperature was completed at NPL during June and July 2016. The objectives of the 2016 comparison were to establish the “degree of equivalence” between terrestrially based IR Cal/Val measurements made in support of satellite observations of the Earth’s surface temperature and to establish their traceability to SI units through the participation of National Metrology Institutes (NMIs). During the 2016 comparison, NPL acted as the pilot laboratory and provided traceability to SI units during laboratory comparisons. Stage 1 consisted of Lab comparisons, and took place at NPL during the week starting on 20<sup>th</sup> June 2016. This Stage involved laboratory measurements of participants’ blackbodies calibrated using the NPL reference transfer radiometer (AMBER) and the PTB infrared radiometer, while participants’ radiometers were calibrated using the NPL ammonia heat-pipe reference blackbody. Stage 2 took place at Wraysbury reservoir during the week starting on 27<sup>th</sup> June 2016 and involved field measurements of the temperature of the surface of the reservoir water. Stage 2 also included the testing of the same radiometers alongside each other, completing direct daytime and night-time measurements of the surface temperature of the water. Stage 3 took place in the gardens of NPL during the week starting on 4<sup>th</sup> July 2016 and involved field measurements of the temperature of the surface of a number of solid targets. Stage 3 included the testing of the same radiometers alongside each other, completing direct daytime and night-time measurements of the surface temperature of targets, including short grass, clover, soil, sand, gravel and tarmac/asphalt. This report provides the results of Stage 2, together with uncertainties as provided by the participants, for the comparison of the participants’ radiometers. During the 2016 comparison, all participants were encouraged to develop uncertainty budgets for all measurements they reported. All measurements reported by the participants, along with their associated uncertainties, were analysed by the pilot laboratory and are presented in this report.



© NPL Management Ltd, 2017

ISSN: 2059-6030

National Physical Laboratory  
Hampton Road, Teddington, Middlesex, TW11 0LW

Extracts from this report may be reproduced provided the source is acknowledged  
and the extract is not taken out of context.

Approved on behalf of NPLML by Teresa Goodman, Earth Observation, Climate and  
Optical Group



## Contents

1	<b>INTRODUCTION .....</b>	<b>1</b>
2	<b>ORGANISATION OF THE COMPARISON.....</b>	<b>1</b>
3	<b>3 PARTICIPANTS' RADIOMETERS AND MEASUREMENTS .....</b>	<b>2</b>
	<b>3.1 MEASUREMENTS MADE BY VALENCIA UNIVERSITY .....</b>	<b>6</b>
	3.1.1 Description of Radiometer and Route of Traceability (supplied by Raquel Nicolòs of the University of Valencia).....	6
	3.1.2 Uncertainty Contributions Associated with the WST Measurements at Wraysbury Reservoir .....	9
	3.1.3 Valencia University WST measurements at Wraysbury reservoir .....	11
	<b>3.2 MEASUREMENTS MADE BY JPL .....</b>	<b>13</b>
	3.2.1 Description of the radiometer and route of traceability .....	13
	<b>3.2.2</b> Uncertainty contributions associated with JPL's measurements at NPL.....	13
	3.2.3 JPL radiometer WST measurements at Wraysbury reservoir.....	13
	<b>3.3 MEASUREMENTS MADE BY KIT .....</b>	<b>15</b>
	3.3.1 Description of radiometer and route of traceability .....	15
	3.3.3 KIT WST obtained from KT15.85 IIP radiometer measurements .....	17
	<b>3.4 MEASUREMENTS MADE BY CSIRO.....</b>	<b>18</b>
	3.4.1 Description of Radiometer and route of traceability .....	18
	3.4.2 Uncertainty contributions associated with CSIRO's WST measurements .....	19
	3.4.3 CSIRO ISAR 5D measurements of Wraysbury reservoir .....	19
	<b>3.5 MEASUREMENTS MADE BY GOTA.....</b>	<b>21</b>
	3.5.1 Description of radiometer and route of traceability.....	21
	3.5.2 Uncertainty contributions associated with GOTA's measurements at NPL.....	23
	3.5.3 WST Measurements made by the GOTA CE312-2 radiometer .....	24
	<b>3.6 MEASUREMENTS MADE BY STFC RAL.....</b>	<b>25</b>
	3.6.1 Description of the radiometer and route of traceability .....	25
	3.6.2 Uncertainty contributions associated with STFC RAL's measurements at NPL .....	26
	3.6.3 STFC RAL SISTeR measurements of Wraysbury reservoir surface temperature .....	27
	<b>3.7 MEASUREMENTS MADE BY SOUTHAMPTON UNIVERSITY.....</b>	<b>28</b>
	3.7.1 Description of radiometer and route of traceability.....	28
	3.7.2 Uncertainty contributions associated with UoS' measurements at NPL .....	29
	3.7.3 UoS ISAR measurements of Wraysbury reservoir surface temperature .....	29
	<b>3.8 MEASUREMENTS MADE BY DMI .....</b>	<b>31</b>
	3.8.1 Description of radiometers and route of traceability .....	31
	3.8.2 Uncertainty contributions associated with DMI's ISAR measurements at NPL .....	31
	3.8.3 DMI ISAR radiometer WST measurements of Wraysbury reservoir.....	32
	3.8.4 Additional comments from institute .....	34
	<b>3.9 MEASUREMENTS MADE BY OUC, QINGDAO .....</b>	<b>34</b>
	3.9.1 Description of radiometers and route of traceability .....	34
	3.9.2 Uncertainty contributions associated with OUC's measurements at NPL .....	35
	3.9.3 OUC's radiometer measurements of the WST at Wraysbury reservoir. ....	37



4 **SUMMARY OF THE RESULTS.....40**

5 **DISCUSSION.....45**

**5.1 RADIOMETER POSITIONING AT TEST SITE ..... 45**

**5.2 WEATHER AND AUTOMATION DURING CAMPAIGN..... 45**

**5.3 THE EFFECT OF THE WIND..... 46**

6 **CONCLUSIONS AND LESSONS LEARNT.....47**

## 1 INTRODUCTION

The measurement of the Earth's surface temperature and, more fundamentally, its temporal and spatial variation, is a critical operational product for meteorology and an essential parameter for climate monitoring. Satellites have been monitoring global surface temperature for some time. However, it is essential for long-term records that such measurements are fully anchored to SI units.

Field-deployed infrared radiometers<sup>1</sup> currently provide the most accurate surface-based measurements which are used for calibration and validation of Earth observation radiometers. These radiometers are in principle calibrated traceably to SI units, generally through a blackbody radiator. However, they are of varying design and are operated by different teams in different parts of the globe. It is essential for the integrity of their use, that any differences in their measurements are understood, so that any potential biases are removed and are not transferred to satellite sensors.

A comparison of terrestrial based infrared (IR) radiometric instrumentation used to support calibration and validation of satellite borne sensors with emphasis on sea/water surface temperature was completed in Miami in 2001 (Barton et al., 2004) (Rice et al., 2004) and at NPL and Miami in 2009 (Theocharous and Fox, 2010) (Theocharous et al., 2010). However, seven years had passed, and as many of the satellite sensors originally supported were nearing the end of their life, a similar comparison was repeated in 2016. The objectives of the 2016 comparison were to establish the "degree of equivalence" between terrestrially based IR Cal/Val measurements made in support of satellite observations of the Earth's surface temperature and to establish their traceability to SI units through the participation of NMIs.

## 2 ORGANISATION OF THE COMPARISON

During the 2016 comparison, NPL acted as the pilot laboratory and, with the aid of PTB, provided traceability to SI units during laboratory comparisons at NPL and was supported with specialist application advice from University of Southampton, RAL and KIT. The 2016 comparison consisted of three stages. Stage 1 took place at NPL in June 2016 and involved laboratory measurements of participants' blackbodies calibrated using the NPL reference transfer radiometer (AMBER) (Theocharous et al., 1998) and the PTB infrared radiometer, while the performance of the participants' radiometers was compared using the NPL ammonia heat-pipe reference blackbody. The performance of 8 blackbodies and 19 radiometers operating on 24 measurement channels was compared during Stage 1. Stage 2 took place on the platform which is located in the middle of Wraysbury reservoir in June/July 2016. The performance of 9 radiometers operating on 14 measurement channels was compared during Stage 2. Stage 2 included the testing of the participating radiometers alongside each other, completing direct daytime and night-time measurements of the skin temperature of the reservoir water. Stage 3 took place in the gardens of NPL during the week starting on 4<sup>th</sup> July 2016 and involved field measurements of the temperature of the surface of a number of solid targets. Stage 3 included the testing of the same radiometers alongside each other, completing direct daytime and night-time measurements of the surface temperature of targets, including short grass, clover, soil,

---

<sup>1</sup> This report describes the comparison of instruments which are referred to by participants as "radiometers". However, radiometers generally measure and report radiometric parameters in radiometric units (W, Wm<sup>-2</sup>, etc.). The instruments dealt with here measure temperature (in units of degrees C units or K) so they are thermometers or "radiation thermometers". However, in view of the common usage of the terminology for this application, this report will continue to use the term "radiometer".

sand, gravel and tarmac/asphalt.

This report provides the results, together with uncertainties as provided by the participants, of the water surface temperature measurements taken over a 5 day period during the week beginning 27<sup>th</sup> June 2016, made at the NPL facility at Wraysbury reservoir. The laboratory comparisons of the participants' blackbodies, as measured by the NPL AMBER radiometer and the PTB infrared radiometer, and the comparison of the participants' radiometers against the NPL ammonia heat-pipe blackbody, as well as the LST comparison that took place in the NPL gardens, are presented in other reports (Theocharous et al. 2017a, Theocharous et al. 2017b, Barker Snook et al. 2017).

During the 2016 comparison, all participants were encouraged to develop uncertainty budgets for all measurements they reported. In order to achieve optimum comparability, lists containing the principal influence parameters for the measurements were provided to all participants. All measurements reported by the participants, along with their associated uncertainties, were analysed by the pilot laboratory and are presented in this report.

### **3 PARTICIPANTS' RADIOMETERS AND MEASUREMENTS**

The 2016 water surface temperature radiometer comparison was completed with the participating radiometers mounted on the NPL platform which is located in the middle of Wraysbury water reservoir, Middlesex, UK. Figure 3.1 shows a photo of Wraysbury reservoir with the platform from which the measurements were made positioned in the middle of the reservoir. Access to the platform was by boat only.

Nine organisations with ten radiometers participated in the 2016 WST comparison at Wraysbury reservoir. The east side of the platform had rigid rails running along part of its length so all participating radiometers were attached to the rails on the east side of the platform. Figure 3.2 shows the radiometers mounted along the rails on the platform on Wraysbury reservoir, while Figure 3.3 shows another view of the radiometers mounted on the platform at Wraysbury reservoir.



Figure 3.1: Wraysbury reservoir with the platform on which the radiometers were mounted located in the middle of the reservoir.



Figure 3.2: The radiometers were mounted along the rails on the east side of the platform.



Figure 3.3: Another view of the participating radiometers mounted on the platform at Wraysbury reservoir.

A thermal imager was used to provide a record of the temperature distribution of the surface temperature of the water at the location where the radiometers were viewing the water. Figure 3.4 shows the thermal imager viewing the surface of the water next to the location where the radiometers were mounted. The thermal imager responded to wavelengths in the  $8\ \mu\text{m}$  to  $12\ \mu\text{m}$  range. Figure 3.5 shows an example of a thermal image of the surface of the water of the reservoir and shows that the instantaneous surface temperature of the water varied by approximately a couple of degrees C. The variations in the surface temperature was on the same time scale and spatial scale as the ripples which were present on the surface of the water. These ripples, which can be clearly seen in Figure 3.4, are believed to give rise to the temperature fluctuations which were recorded by the thermal imager. The ripples give rise to real temperature changes due to the cycling of the water from below the surface but they also alter the specular reflections of the sky/clouds due to the constant changing of the shape of the surface of the water. Since the Field of View (FoV) of the participating radiometers was comparable to that of the thermal imager, and the effective temporal response the radiometers was much slower than the cycling time of the ripples/temperature of the surface of the water, it can be concluded that the radiometers were measuring the time average and space average of the surface temperature fluctuations of the water in their FoV.



Figure 3.4: The thermal imager viewing the surface of the water. Note the ripples on the surface of the water which give rise to the temperature fluctuation which were observed in the thermal images recorded.

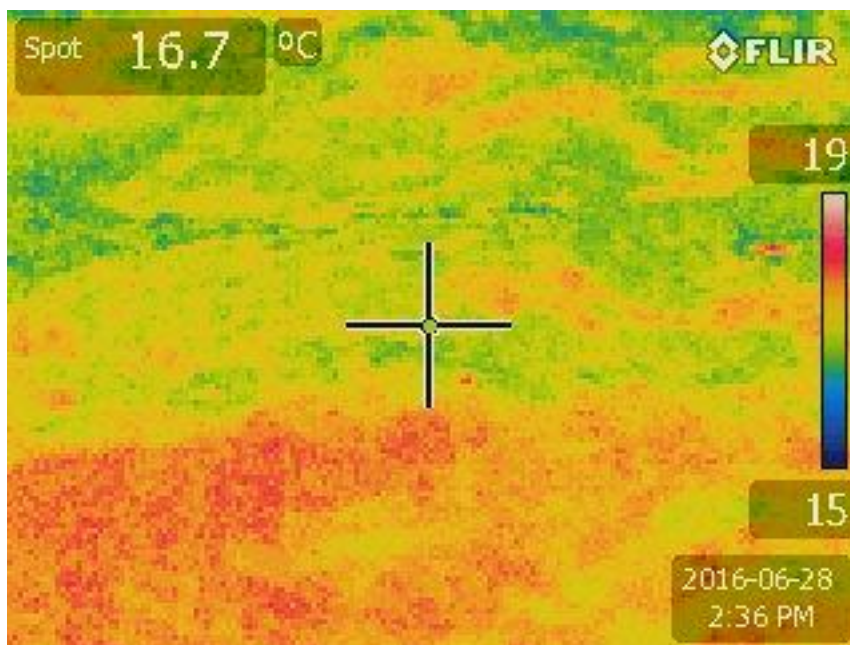


Figure 3.5: Thermal image of the surface of the water at Wraysbury reservoir indicating that the instantaneous apparent surface temperature varied by approximately a couple of degrees.

Section 3 gives brief descriptions of the radiometers participating in the water surface temperature comparison at Wraysbury reservoir and gives the measurements which were completed by the participating radiometers during these comparisons, along with the

corresponding combined uncertainty values which were provided by the participants. Section 3 also provides the uncertainty budgets of the measurements completed by the participating radiometers, as provided by the participants. In some cases the level of detail provided by participants in the uncertainty budgets of their measurements is fairly limited and not ideal. However, whatever was provided by the participants is included in this report, along with a summary of the results for each participant for each stage of the comparison.

Section 3 also provides plots of the difference of the WST measurements provided by each participant and the mean of the measurements provided by all participants at that time. Ideally the mean should be determined from the measurements of the participating radiometers, weighted by their uncertainties. However, to do this required a full breakdown of uncertainties so that the weights can be fully evaluated and agreed upon by participants in advance. This was not possible from the data provided by some participants. The approach which was adopted uses the simple mean of the radiometer measurements.

### 3.1 MEASUREMENTS MADE BY VALENCIA UNIVERSITY

Dept. of Earth Physics and Thermodynamics, University of Valencia.  
50, Dr. Moliner. ES-46100, Burjassot (Valencia), Spain  
Contact Names: César Coll and Raquel Niclòs

#### 3.1.1 Description of Radiometer and Route of Traceability (supplied by Raquel Niclòs of the University of Valencia)

Make and type of Radiometer: **CIMEL Electronique CE312-2, six spectral bands (two units)**

**Outline technical description of instrument:** Type of detector: thermopile, operating at ambient temperature. Six spectral bands: B1 8.0-13.3  $\mu\text{m}$ , B2 10.9-11.7  $\mu\text{m}$ , B3 10.2-11.0  $\mu\text{m}$ , B4 9.0-9.3  $\mu\text{m}$ , B5 8.5-8.9  $\mu\text{m}$ , and B6 8.3-8.6  $\mu\text{m}$ . Broad band: Germanium window and zinc sulphide filters. Narrow bands: interference filters. Field of view: 10°. The instrument has a built-in radiance reference made of a concealable gold-coated mirror which enables comparison between the target radiance and the reference radiation from inside the detector cavity. The temperature of the detector is measured with a calibrated PRT, thus allowing compensation for the cavity radiation. The relevant outputs of the radiometer are the detector temperature and the difference in digital counts between the signals from the target and the detector cavity.

**Operational methodology during measurement campaign:** Specular reflection is approximated for the water surface reflection. This is the usual approximation for the water surface (Barton et al., 1989) without foam coverage (Niclòs et al. 2007). The reflection term can be rewritten as:

$$L_i^{ref}(\theta, \phi) = [1 - \varepsilon_i(\theta, \phi)]L_{i\ atm}^\downarrow(\theta, \phi \pm \pi)$$

and the radiometer observing the water surface at a zenith angle ( $\theta$ ) measures:

$$L_i(\theta, \phi) = \varepsilon_i(\theta, \phi)B_i(T) + L_i^{ref}(\theta, \phi)$$

**The CE312-2 Band 3** (responding in the 10.2-11.0  $\mu\text{m}$  wavelength range) was selected for the WST measurements since this channel requires the lowest emissivity and atmospheric corrections (Nicolòs et al., 2004). A viewing angle of  $25^\circ$  was used to reduce the emissivity correction uncertainties but also the influence of the platform. The CE312-2 Unit 2 measured the water surface radiance at  $25^\circ$  (from Nadir) and the CE312-2 Unit 1 measured directly and simultaneously the downwelling sky radiance at  $25^\circ$  (from Zenith).

### 3.1.2 Establishment or traceability route for primary calibration including date of last realization and breakdown of uncertainty:

The following calibration error analysis is based on laboratory measurements with the Landcal blackbody P80P (total uncertainty of 0.34 K; Laboratory Appendixes B and E) on May 13-18, 2016, and estimates from the references. Blackbody measurements were taken at six fixed temperatures (0-50  $^\circ\text{C}$ ) in two different runs with instrument realigning. The values reported below are typical values for all blackbody temperatures considered for **band 3** (units 1 and 2).

#### Uncertainty contributions:

The CE312-2 band 3 (10.2-11.0  $\mu\text{m}$ ) was selected for the WST comparison.

Several parameters were varied for the uncertainty analysis, with the following ranges:

- A. Water surface temperatures from 289.7 to 291.7 K.
- B. Sky temperatures from 233 to 278 K.
- C. Wind speeds from 0 m/s to 15 m/s.
- D. Zenith angle from  $22.5^\circ$  to  $27.5^\circ$ .

These values are representative of the measurement conditions during the WST comparison.

#### Type A

- **Repeatability:** Typical value of the standard deviation of 15 measurements at fixed black body temperature without re-alignment of radiometer.

<b>Unit 1</b>	<b>B3</b>
<b>K</b>	0.04
<b>% (at 300 K)</b>	0.012

<b>Unit 2</b>	<b>B3</b>
<b>K</b>	0.03
<b>% (at 300 K)</b>	0.009

- **Reproducibility:** Typical value of difference between two runs of radiometer measurements at the same blackbody temperature including re-alignment.

<b>Unit 1</b>	<b>B3</b>
<b>K</b>	0.08
<b>% (at 300 K)</b>	0.025

<b>Unit 2</b>	<b>B3</b>
<b>K</b>	0.06



<b>% (at 300 K)</b>	0.019
---------------------	-------

Total Type A uncertainty (RSS):

<b>Unit 1</b>	<b>B3</b>
<b>K</b>	0.08
<b>% (at 300 K)</b>	0.028

<b>Unit 2</b>	<b>B3</b>
<b>K</b>	0.06
<b>% (at 300 K)</b>	0.021

### **Type B**

- **Primary calibration:** 0.34 K (estimation of the total uncertainty of the Landcal blackbody P80P).

- **Water emissivity:** 0.15 K. Emissivity values were computed following the methodology proposed by Niclos et al. (2009) based on the model of Wu and Smith (1997) for sea surface. Water salinity does not affect the water surface emission and its angular variation in the region from 8 to 13  $\mu\text{m}$  (Salisbury & D'Aria, 1992; Niclòs & Caselles, 2008), with negligible differences between fresh and sea water emissivities, mainly for the CE312 band 3 spectral range. Spectral values were integrated for the radiometer band (using the response function provided by the manufacturer) to obtain the band emissivity against wind speed and observation angle. A water emissivity uncertainty of 0.004 was considered for the analysis (Niclòs et al. 2005, 2014). Downwelling sky radiances were directly measured by the CE312-2 Unit 1 (band 3). The radiometer total uncertainty of 0.36 K could be considered for this term. In this case the water emissivity uncertainty would be of 0.11 K. However, an uncertainty of 30% in the downwelling sky radiance was used for the analysis, due to the partially cloudy and very variable sky conditions during the campaign. Although the downwelling sky radiance effect is relatively small, these sky conditions were not optimum for the WST comparison. We usually use cloud-free sky conditions for CAL/VAL activities.

- **Water surface “roughness”:** 0.005 K. This term is related with wind speed. Surface wind produces roughness on the water surface, which can be characterized using an approximately normal and isotropic facet slope distribution. Wu and Smith (1997) considered this facet slope distribution to model the sea surface emissivity under several wind speed conditions, taking into account also the effect of multiple surface reflections. A wind speed uncertainty of 5 m/s was considered for the analysis. The wind speed effect is really low at a zenith angle of 25°.

- **Angle of view to nadir:** 0.005 K. A zenith angle uncertainty of 2.5° was considered for the analysis, even though we used a digital inclinometer (with a sensitivity of 0.1°) to set up the radiometers.

- **Linearity of radiometer:** 0.06 K (Typical value for all bands in the temperature range 0 °C to 40 °C according to Legrand et al. (2000)).

- **Drift since calibration:** 0.05 K. It has been corrected for using the calibration measurements performed with the Landcal blackbody P80P mentioned above. A linear correcting equation has been derived for each band and radiometer, with the radiometer measured temperature and the detector temperature as inputs. The uncertainty for this correction is the RSS of the typical estimation uncertainty of the linear regression (0.05 K for unit 1 and 0.04 K for unit 2) and the uncertainties resulting from the propagation of input temperature errors (standard deviations for 15 measurement at a fixed temperature) in the linear correcting equation. The resulting uncertainty in the correction of calibration drift is 0.07 K for unit 1 and 0.05 K for unit 2.

**Ambient temperature fluctuations:** 0.04 K. The effect of ambient temperature fluctuations is compensated by the CE312 radiometers by measuring the detector cavity temperature by means of a calibrated PRT. The uncertainty in this process is the uncertainty of the internal PRT, which is 0.04 K according to Legrand et al. (2000).

**Atmospheric absorption/emission:** 0.00013 K. A vertical distance of 1 m was considered between the radiometer and the water surface for the analysis; although the actual distance was lower (around 30 cm). Atmospheric parameters (transmittances and upwelling radiances) were simulated with the MODTRAN 5 radiative model and NCEP atmospheric profiles suitable for the campaign conditions. A zenith angle of 25° was considered for the analysis.

Type A + Type B uncertainty (RSS): **0.39 K**.

### **Uncertainty Contributions Associated with the WST Measurements at Wraysbury**

#### **Reservoir**

Table 3.1 summarises the uncertainties which are involved in the measurement of the WST at Wraysbury reservoir. It should be noted that some of these components may sub-divide further depending on their origin. The RMS total refers to the usual expression i.e. square root of the sum of the squares of all the individual uncertainty terms as shown in the example for Type A uncertainties.

**Table 3.1: Summary the uncertainties which are involved in the measurement of the WST at Wraysbury reservoir.**

<b>Uncertainty Contribution</b>	<b>Type A Uncertainty in Value / %</b>	<b>Type B Uncertainty in Value / (appropriate units)</b>	<b>Uncertainty in Brightness temperature K</b>
<b>Repeatability of measurement</b>	0.03 K / 0.009 %		0.03
<b>Reproducibility of measurement</b>	0.06 K / 0.019 %		0.06
<b>Primary calibration</b>			0.34
<b>Water emissivity</b>		0.004 in emissivity, 30% in sky radiance (CE 312 unit 1, band 3)	0.15
<b>Water surface “roughness”</b>		5 m/s in wind speed	0.005
<b>Angle of view to nadir</b>		2.5° in viewing angle	0.005
<b>Linearity of radiometer</b>			0.06
<b>Drift since last calibration</b>			0.05
<b>Ambient temperature fluctuations</b>			0.04
<b>Atmospheric absorption/emission</b>			0.00013
<b>RMS total</b>	0.06 K / 0.021 %		0.39

**Radiometer usage (deployment), previous use of instrument and planned applications:**

The CE312 radiometers and methodologies have been used (Nicolòs et al., 2004, 2005, 2007, 2008, 2014, 2015) and will be used for CAL/VAL activities and emissivity characterizations in the framework of different research projects.

### References associated with Section 3.1:

- Legrand, M., C. Pietras, G. Brogniez, M. Haeffelin, N. K. Abuhassan and M. Sicard (2000). A high-accuracy multiwavelength radiometer for in situ measurements in the thermal infrared. Part I: characterization of the instrument, *J. Atmos. Ocean Techn.*, 17, 1203-1214.
- Niclos, R., Caselles, V., Coll, C., Valor, E., and Rubio, E. (2004). Autonomous Measurements of Sea Surface Temperature Using In Situ Thermal Infrared Data. *Journal of Atmospheric and Oceanic Technology*, 21: 683-692.
- Niclos, R., Valor, E., Caselles, V., Coll, C., and Sanchez, J.M. (2005). In situ angular measurements of thermal infrared sea surface emissivity – Validation of models. *Remote Sensing of Environment*, 94: 83-93.
- Niclòs, R., Caselles, V., Valor, E., and Coll, C. (2007). Foam effect on the sea surface emissivity in the 8–14  $\mu\text{m}$  region. *Journal of Geophysical Research – Oceans*, 112, Issue C12.
- Niclòs, R., and Caselles, V. (2008). Water salinity and foam coverage effects on thermal-infrared sea surface emissivity. In: *Ocean Remote Sensing: Recent Techniques and Applications*. Ed. Research Singpost.
- Niclòs, R., Caselles, V., Valor, E., Coll, C. and Sanchez, J. M. (2009). A simple equation for determining the sea surface emissivity in the 3–15  $\mu\text{m}$  region. *Int. J. Remote Sens.*, vol. 30, no. 6, pp. 1603–1619.
- Niclos, R., Doña, C., Valor, E., & Bisquert, M. (2014). Thermal-Infrared Spectral and Angular Characterization of Crude Oil and Seawater Emissivities for Oil Slick Identification. *IEEE Transactions on Geoscience and Remote Sensing*, Vol. 52 (9), 5387- 5395.
- Niclòs, R., Valiente, J.A., Barberà, M.J., Coll, C. (2015). An Autonomous System to Take Angular Thermal-Infrared Measurements for Validating Satellite Products. *Remote Sensing*, 7, 15269-15294. <http://www.mdpi.com/2072-4292/7/11/15269>.
- Salisbury, J. W. and D'Aria, D. M. (1992). Emissivity of terrestrial materials in the 8-14 micrometer atmospheric window. *Remote Sensing of Environment*, 42, 83-106.
- Sicard, M., Spyak, P. R., Brogniez, G., Legrand, M., Abuhassan, N. K., Pietras, C., and Buis, J. P. (1999). Thermal infrared field radiometer for vicarious cross-calibration: characterization and comparisons with other field instruments. *Optical Engineering*, 38 (2), 345-356.
- Wu, X. and Smith, W.L. (1997). Emissivity of rough sea surface for 8-13  $\mu\text{m}$ : modelling and verification. *Applied Optics*, 36: 2609-2619.

#### 3.1.3 Valencia University WST measurements at Wraysbury reservoir

Figure 3.1.1 shows the WST obtained from UoV CIMEL CE312-2 radiometer measurements when it was viewing the surface of Wraysbury reservoir over the five-day measurement period. The uncertainty bars (shown in orange) represent the uncertainty values provided by UoV, which correspond to the WST measurements shown in the Figure. Figure 3.1.2 shows the difference of the measurements of the WST obtained by UoV and the mean of all measurements, over the five-day measurement period.

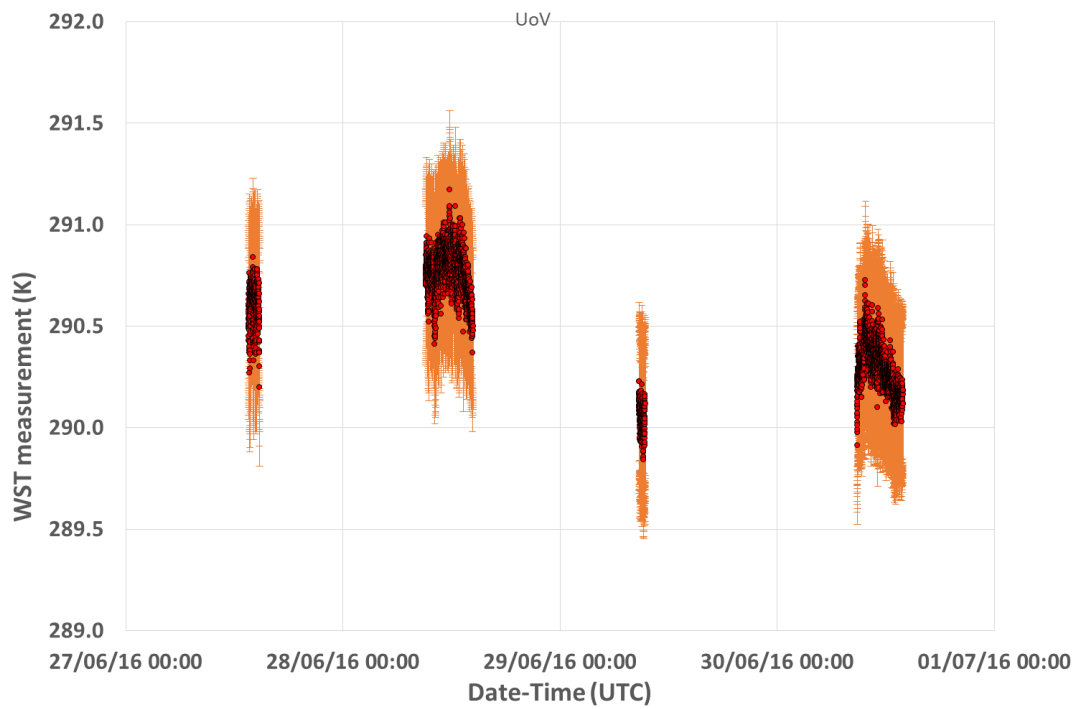


Figure 3.1.1: Measurements of the water surface temperature of Wraysbury reservoir made by the UoV CIMEL CE312-2 radiometer.

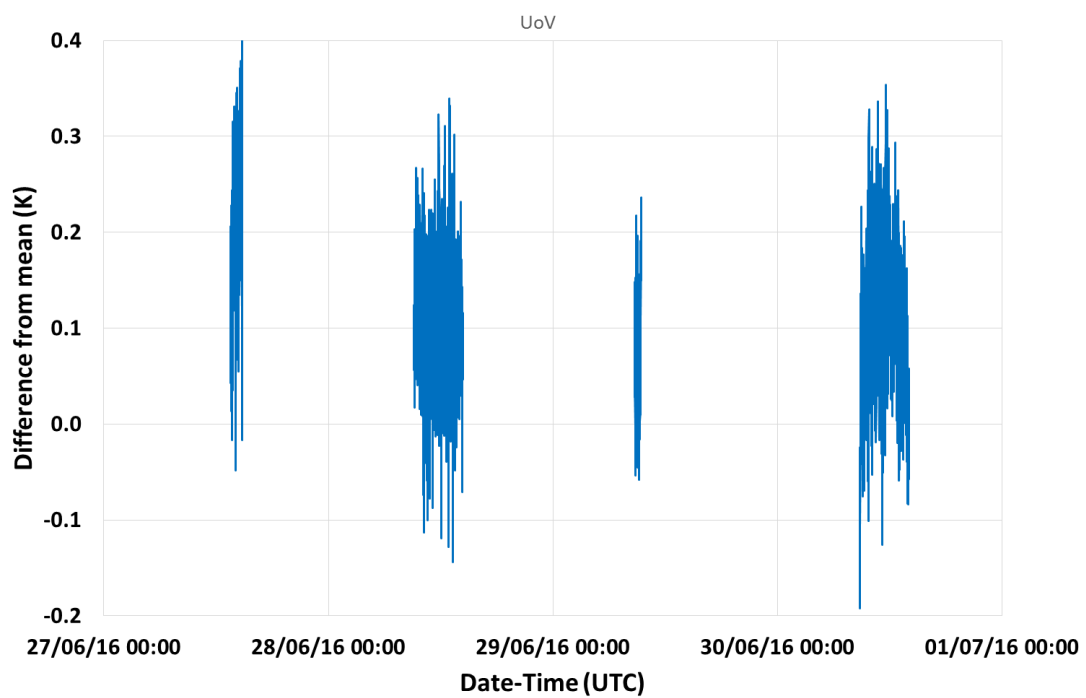


Figure 3.1.2: Difference of the water surface temperature (WST) of Wraysbury reservoir obtained by UoV and the mean of the WST provided by the 10 participants, over the five-day measurement period.

## 3.2 MEASUREMENTS MADE BY JPL

NASA/Jet Propulsion Laboratory  
California Institute of Technology  
Contact Name: Gerardo Rivera

### 3.2.1 Description of the radiometer and route of traceability

The description of the JPL radiometer can be found on: <http://calval.jpl.nasa.gov/radiometers>

An Apogee SI-121 radiometer is used within the JPL participating Radiometer. The Apogee SI-121 Radiometer is considered a narrow field-of-view infrared radiometer sensor with an 18 degree half-angle and a response time of 0.6 seconds.

The Measurement Repeatability of the JPL radiometer is less than 0.05 °C.

The Stability (Long-term Drift) of the JPL radiometer is less than 2% change in slope per year when the germanium filter is maintained in a clean condition

The Response Time of the JPL radiometer is 0.6 s. Response Time is defined as the time for detector signal to reach 95 % following a step change of the input.

The Spectral Range of the radiometer extends over the 8 μm to 14 μm atmospheric window

The Operating Environment of the radiometer is from -55 °C to 80 °C, over the 0 to 100 % relative humidity range.

### 3.2.2 Uncertainty contributions associated with JPL's measurements of WST

Ali Abtahi of JPL has clarified the uncertainty of the JPL Radiometer. The uncertainty of the JPL radiometer is based on the uncertainty of the Apogee radiometer (on which the JPL radiometer is based) but the uncertainty also depends on the platinum thermoelectric (TE) modules which are also used within the JPL radiometer.

The uncertainty value which should be used with the JPL radiometer is 0.1 °C when measurements in the temperature range -10 °C to +60 °C are being made in ambient temperature environments of +4 °C to +44 °C.

### 3.2.3 JPL radiometer WST measurements at Wraysbury reservoir

Figure 3.2.1 shows the output of the JPL radiometer when it was viewing the surface of Wraysbury reservoir over five days. The uncertainty bars in the figure represent the uncertainty values provided by JPL which correspond to the measurements shown in the Figure. Figure 3.2.2 shows the difference of the measurements of the WST obtained by JPL and the mean of all measurements, over the five-day measurement period.

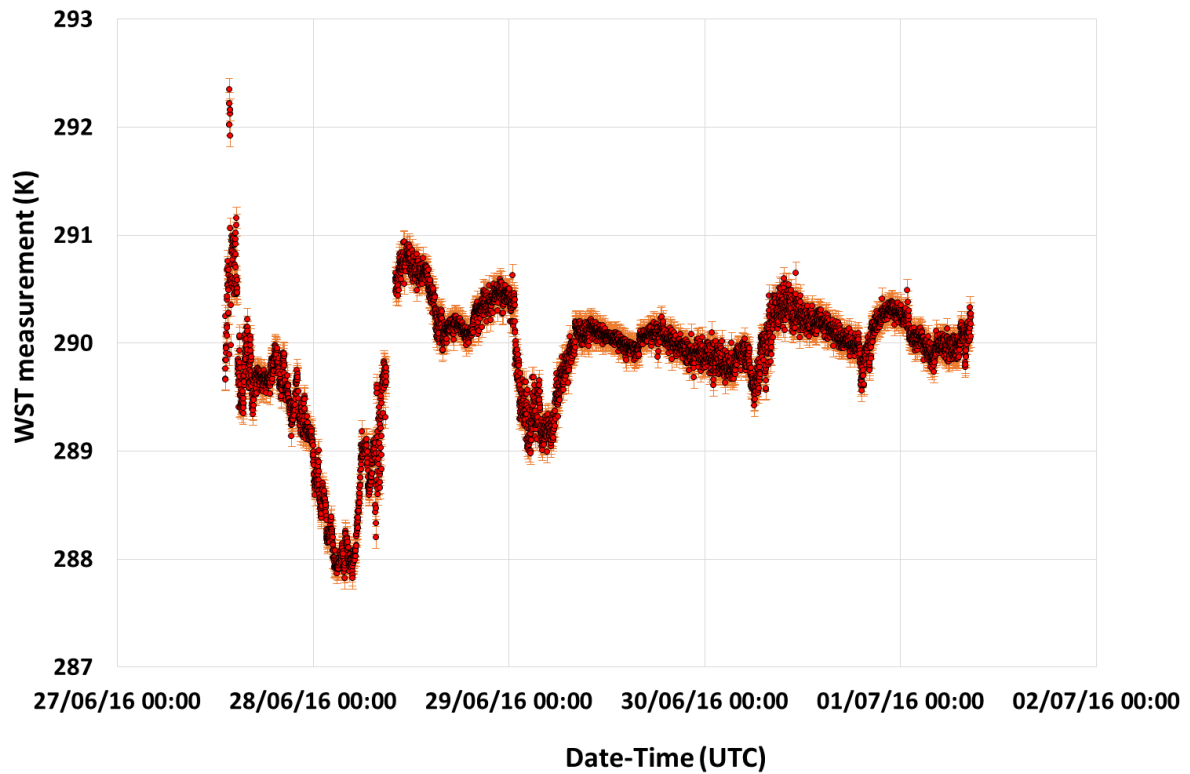


Figure 3.2.1: Measurements of the water surface temperature of Wraysbury reservoir made by the JPL radiometer.

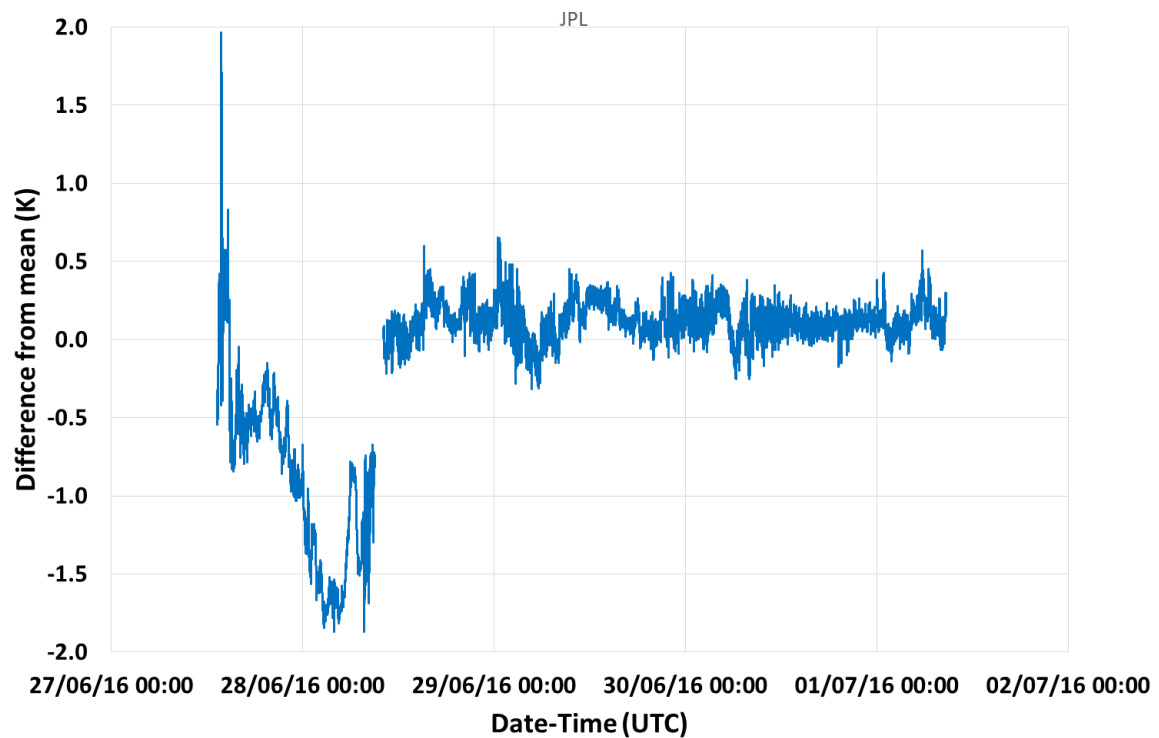


Figure 3.2.2: Difference of the water surface temperature (WST) of Wraysbury reservoir obtained by JPL and the mean of the WST provided by the 10 participants, over the five-day measurement period.

### 3.3 MEASUREMENTS MADE BY KIT

IMK-ASF, Karlsruhe Institute of Technology (KIT)  
Hermann-von-Helmholtz-Platz 1, 76344 Eggenstein-Leopoldshafen, Germany  
Contact Name: Dr. Frank-M. Goettsche.

#### 3.3.1 Description of radiometer and route of traceability

**Make and type of Radiometer:** Heitronics KT15.85 IIP with L6 lens ([www.heitronics.com](http://www.heitronics.com))

**Outline technical description of instrument:** The KT15.85 IIP is a single channel radiometer based on a pyroelectric infrared detector. This type of sensor links radiance measurements via beam-chopping to internal reference temperature measurements and thermal drift can practically be eliminated. The KT15.85 IIP covers the spectral range from 9.6  $\mu\text{m}$  to 11.5  $\mu\text{m}$ , has an uncertainty of about 0.3 K over the temperature range relevant to land surfaces and offers excellent long-term stability. The response time of the surface observing radiometer (serial #11650) was set to 10 sec and its temperature range to -25  $^{\circ}\text{C}$  to +100  $^{\circ}\text{C}$ . The type L6 lens used has a full-view angle of 8.3 $^{\circ}$  and is well-suited for directional measurements.

#### **Establishment of traceability route for primary calibration including date of last realisation and breakdown of uncertainty.**

Primary calibrations to within specifications were performed on the 03.07.2015 (serial #11650) and 05.05.2015 (serial #11615) by Heitronics GmbH, Wiesbaden, Germany. Breakdowns of uncertainties are not available.

#### **Operational methodology during measurement campaign:**

During the Water Surface Temperature (WST) experiments at Wraysbury Reservoir the KT15.85 IIP radiometer was mounted about 50 cm above the water surface. Together with a nadir view angle of 45 $^{\circ}$  this yielded a FOV diameter of about 10 cm. The second KT15.85 IIP radiometer (serial #11615, temperature range -100  $^{\circ}\text{C}$  to +100  $^{\circ}\text{C}$ ) simultaneously measured down-welling ‘sky’ radiance at the complementary angle (45 $^{\circ}$  zenith angle). Measurements were taken every 10 sec by a Campbell Scientific CR1000 data logger and averaged over 1 minute. Water surface emissivity at 10.5  $\mu\text{m}$  and for 3 m/s wind speed was taken from Masuda et al. (1988):

Masuda, K., Takashima, T., and Takayama, Y. (1988). Emissivity of Pure Sea Waters for the Model Sea Surface in the Infrared Window Regions. *Remote Sensing of Environment*, Vol. 24, pp. 313-329.

Data processing methods for SST determination and KT15 radiometer spectral characteristics are described in:

Donlon, C., Robinson, I., Reynolds, M., Wimmer, W., Fisher, G., Edwards, R., and Nightingale, T. J. (2008). An Infrared Sea Surface Temperature Autonomous Radiometer (ISAR) for Deployment aboard Volunteer Observing Ships (VOS). *Journal of Atmospheric and Oceanic Technology*, Vol. 25, pp. 93-113.



**Radiometer usage (deployment), previous use of instrument and planned applications.**

The KT15.85 IIP's were used for inter-calibrations at KIT's validation stations Dahra, Senegal and Evora, Portugal. They will be deployed for several years in support of KIT's long-term satellite LST validation activities.

**3.3.2 Uncertainty Contributions to KIT's Water Surface Temperatures (WST) at Wraysbury Reservoir**

<b>Uncertainty Contribution</b>	<b>Type A Uncertainty in Value / %</b>	<b>Type B Uncertainty in Value / (appropriate units)</b>	<b>Uncertainty in Brightness temperature K</b>
<b>Repeatability of measurement</b>	0.12		0.024
<b>Reproducibility of measurement</b>	0.12		0.024
<b>Primary calibration</b>		0.250 K	0.250
<b>Water emissivity</b>		0.1%	0.067
<b>Water surface "roughness"</b>		2.0 m/s	0.033
<b>Angle of view to nadir</b>		2.5 °	0.117
<b>Linearity of radiometer</b>		0.053 K	0.053
<b>Drift since last calibration</b>		0.176 K	0.176
<b>Temperature resolution</b>		0.035 K	0.035
<b>Ambient temperature fluctuations</b>		0.035 K	0.035
<b>Atmospheric absorption/emission</b>		0.035 K	0.035
<b>Down-welling sky radiance</b>		0.004 K	0.004
<b>RMS total</b>	0.173		0.347

The reported uncertainty is based on a standard uncertainty (coverage factor  $k=1$ ), providing a confidence level of approximately 68%.

**Comments:**

Emissivity estimates are taken from Masuda et al. (1988) at 10.5  $\mu\text{m}$ , 45° view angle and 3m/s wind speed. Uncertainty estimates assume 15 K temperature difference between water surface and sensor housing. Relative uncertainties are given 'at reading' at 20 °C.

### 3.3.3 KIT WST obtained from KT15.85 IIP radiometer measurements

Figure 3.3.1 shows the WST obtained from KIT Heitronics KT15.85 IIP radiometer measurements when it was viewing the surface of Wraysbury reservoir over the five-day measurement period. The uncertainty bars (shown in orange) represent the uncertainty values provided by KIT, which correspond to the WST measurements shown in the Figure. Figure 3.3.2 shows the difference of the measurements of the WST obtained with the KIT KT15.85 IIP radiometer and the mean of all measurements, over the five-day measurement period.

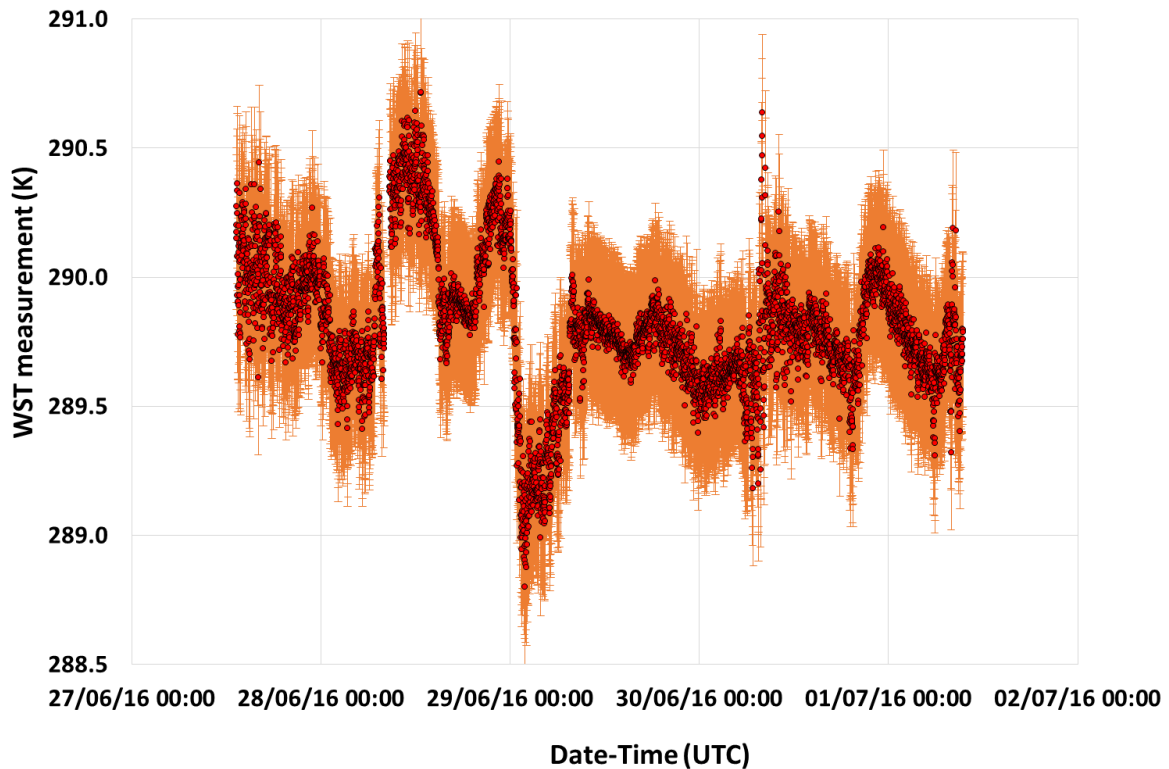


Figure 3.3.1: Water surface temperature (WST) of Wraysbury reservoir obtained with the KIT KT15.85 IIP radiometer.

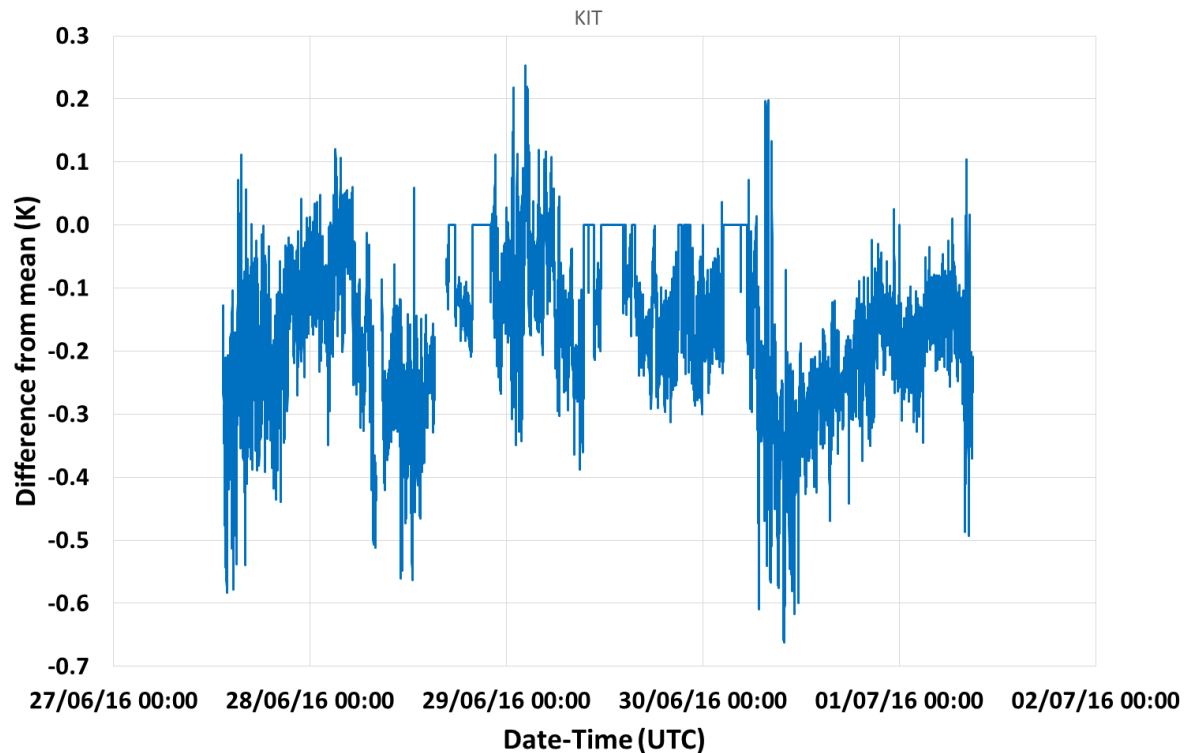


Figure 3.3.2: Difference of the water surface temperature (WST) of Wraysbury reservoir obtained by KIT and the mean of the WST provided by the 10 participants, over the five-day measurement period.

### 3.4 MEASUREMENTS MADE BY CSIRO

Institute/organisation: CSIRO

Ocean Modelling Research Team, Research and Development Branch,  
Bureau of Meteorology GPO Box 1289 Melbourne VIC 3001,  
Level 11, 700 Collins Street, Docklands VIC 3008

Contact Name: Nicole Morgan

Email: [Nicole.Morgan@csiro.au](mailto:Nicole.Morgan@csiro.au)

#### 3.4.1 Description of Radiometer and route of traceability

**Make and type of Radiometer:** ISAR 5D

**Outline Technical description of instrument:**

Full information on this radiometer can be found in: Wimmer, W., and I. Robinson, 2016: The ISAR instrument uncertainty model. *J. Atmos. Oceanic Technol.* doi:10.1175/JTECH-D-16-0096.1, in press.

**Establishment or traceability route for primary calibration including date of last realisation and breakdown of uncertainty:**

Pre workshop calibration completed 22/05/2016.

Post workshop calibration completed 07/08/2016

### Operational methodology during measurement campaign:

Alignment was achieved using an alignment piece specifically designed for the dome nuts on the end to slot into. This is the same way the instrument is aligned during calibration and deployment.

The ISAR runs continuously and the data is post processed using calibration scripts which incorporate the uncertainty model, instrument data and pre and post calibrations to calculate the uncertainty.

### Radiometer usage (deployment), previous use of instrument and planned applications.

This ISAR is installed on RV Investigator, Australia's blue water science vessel. It is part of the underway data collected on every voyage.

### 3.4.2 Uncertainty contributions associated with CSIRO's WST measurements

Table 3.5.2.1 shows the uncertainty budget associated with WST measurements made by the CSIRO radiometer

e	Item	Uncertainty	Unit	Type
1	Detector linearity	<0.01%	K month <sup>-1</sup>	B
2	Detector noise	~0.002	Volts	A
3	Detector accuracy	±0.5	K	B
4	ADC	±1(±76.3)	LSB (μV)	B
5	ADC accuracy	±0.1%	Range	B
6	ADC zero drift	±6	μV °C <sup>-1</sup>	B
7	Reference voltage 16-bit ADC	±15	mV	B
8	Reference voltage 12-bit ADC	±20	mV	B
9	Reference resistor	1	%	B
10	Reference resistor temperature coefficient	±100	Ppm °C <sup>-1</sup>	B
11	BB emissivity	±0.000178	Emissivity	B
12	Sea surface emissivity	±0.07	Emissivity	B
13	Steinhart-Hart approximation	±0.01	K	B
14	Radiate transfer approximation	±0.001	K	B
15	Thermistor	±0.05	K	B
16	Thermistor noise	~0.002	V	A

Sources of uncertainties arising within the ISAR SST retrieval processor. A more detailed breakdown is available in the reference paper "The ISAR instrument uncertainty model".

### 3.4.3 CSIRO ISAR 5D measurements of Wraysbury reservoir

Figure 3.4.1 shows the output of the CSIRO ISAR 5D radiometer when it was viewing the surface of Wraysbury reservoir over the five-day measurement period. The uncertainty bars (shown in brown) represent the uncertainty values provided by CSIRO which correspond to the measurements shown in the Figure. Figure 3.4.2 plots the difference of the measurements of the water surface temperature of Wraysbury reservoir made by the CSIRO ISAR 5D radiometer and the mean of all measurements, over the five-day measurement period.

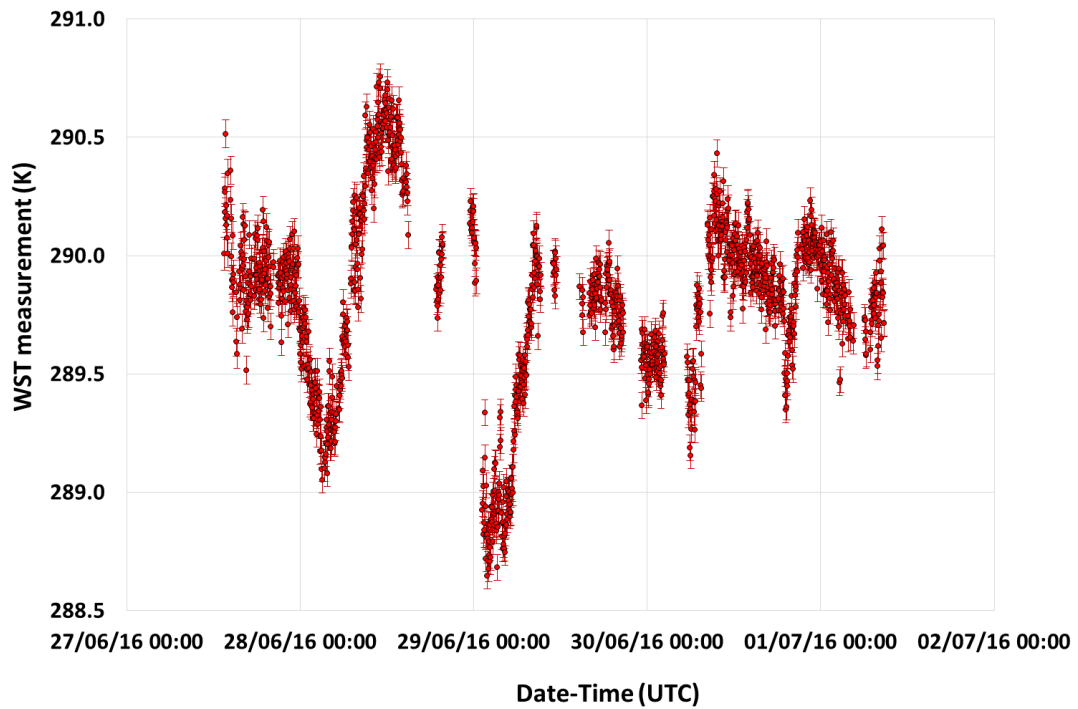


Figure 3.4.1: Measurements of the WST of Wraysbury reservoir made by the CSIRO ISAR 5D radiometer.

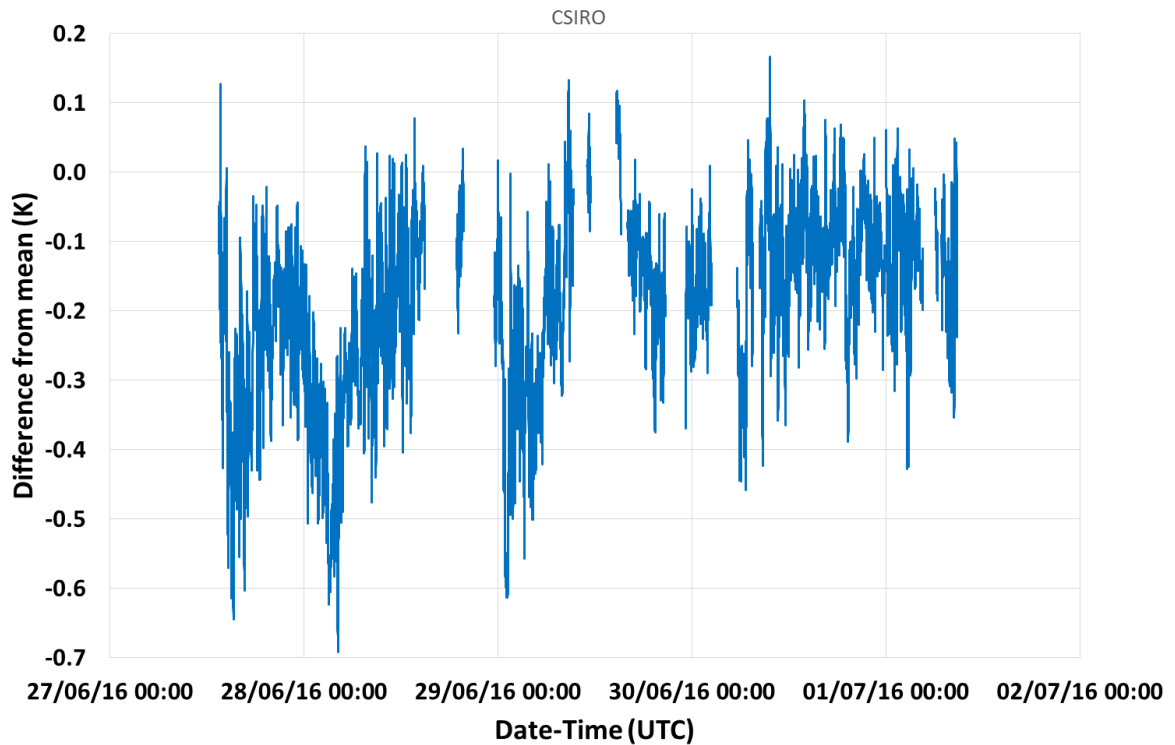


Figure 3.4.2: Difference of the WST of Wraysbury reservoir obtained by the CSIRO ISAR 5D radiometer and the mean of the WST provided by the 10 participants, over the five-day measurement period.

### 3.5 MEASUREMENTS MADE BY GOTA

Institute/organisation: Grupo de Observacion de la Tierra y la Atmosfera (GOTA)  
 Departamento de Física Fundamental y Experimental, Electrónica y Sistemas Universidad de La Laguna Avda. Astrofísico Fco. Sanchez s/n 38200 La Laguna Tenerife, Canarias, Spain.  
 Contact Name: Manuel Arbelo  
 Email: [marbelo@ull.es](mailto:marbelo@ull.es)

#### 3.5.1 Description of radiometer and route of traceability

**Make and type of Radiometer:** CIMEL Electronique CE312-2

**Outline Technical description of instrument:** Type of detector: Thermopile. 6 spectral bands: B1 8-13  $\mu\text{m}$ , B2 11.0-11.7  $\mu\text{m}$ , B3 10.3-11.0  $\mu\text{m}$ , B4 8.9-9.3  $\mu\text{m}$ , B5 8.5-8.9  $\mu\text{m}$ , and B6 8.1-8.5  $\mu\text{m}$ . The spectral characterisation of the instrument can be found in references 1, 2 and 3, below. Broad band: Germanium window and zinc sulphide filters. Narrow bands: interference filters. Field of view: 10°. The instrument has a built-in radiance reference made of a concealable gold-coated mirror which enables comparison between the target radiance and the reference radiation from inside the detector cavity. The temperature of the detector is measured with a PRT, thus allowing compensation for the cavity radiation.

#### References:

1. Sicard, M., Spyak, P. R., Brogniez, G., Legrand, M., Abuhassan, N. K., Pietras, C., and Buis, J. P. (1999), “*Thermal infrared field radiometer for vicarious cross-calibration: characterization and comparisons with other field instruments*”, Optical Engineering, 38 (2), 345-356.
2. M. Legrand, C. Pietras, G. Brogniez, M. Haeffelin, N. K. Abuhassan and M. Sicard (2000) “*A high accuracy multiwavelength radiometer for in situ measurements in the thermal infrared. Part I: characterization of the instrument*”, J. Atmos. Ocean Techn., 17, 1203-1214.
3. <http://www.cimel.fr/?instrument=radiometer-ir-climat-benchmark&lang=en>

#### 3.5.2 Establishment or traceability route for primary calibration including date of last realisation and breakdown of uncertainty

The radiometer has not undergone a traceable primary calibration. The following uncertainty analysis was based on estimates, experience and laboratory measurements with our Landcal Blackbody Source P80P (May 23 to 26, 2016).

Type A

- Repeatability: Typical value of the standard deviation of 10 measurements at fixed black body temperature without re-alignment of radiometer.

	B1	B2	B3	B4	B5	B6	Mean
<b>K</b>	0.04	0.10	0.09	0.09	0.11	0.10	0.09
<b>%</b>	0.01	0.03	0.04	0.03	0.04	0.04	0.03

- Reproducibility: Typical value of difference between two runs of radiometer measurements at the same black body temperature including re-alignment.

	<b>B1</b>	<b>B2</b>	<b>B3</b>	<b>B4</b>	<b>B5</b>	<b>B6</b>	<b>Mean</b>
<b>K</b>	0.05	0.02	0.03	0.03	0.04	0.03	0.03
<b>%</b>	0.01	0.01	0.01	0.01	0.01	0.01	0.01

**Total Type A uncertainty (RSS):**

	<b>B1</b>	<b>B2</b>	<b>B3</b>	<b>B4</b>	<b>B5</b>	<b>B6</b>	<b>Mean</b>
<b>K</b>	0.06	0.10	0.09	0.09	0.12	0.10	0.09
<b>%</b>	0.01	0.03	0.04	0.03	0.04	0.04	0.03

Type B

- Linearity of radiometer: Within temperature range of 278-303 K.

	<b>B1</b>	<b>B2</b>	<b>B3</b>	<b>B4</b>	<b>B5</b>	<b>B6</b>	<b>Mean</b>
<b>K</b>	0.09	0.11	0.10	0.10	0.11	0.10	0.10

- Primary calibration: Typical value of difference between radiometer brightness temperature and Landcal Blackbody Source P80P temperature.

	<b>B1</b>	<b>B2</b>	<b>B3</b>	<b>B4</b>	<b>B5</b>	<b>B6</b>	<b>Mean</b>
<b>K</b>	0.9	0.4	0.3	0.4	0.3	0.2	0.4

- Drift since calibration: 0.0 K (as expected since very recent calibration measurements).

- Ambient temperature fluctuations: 0.3 K

- Size-of-Source Effect: not considered

- Atmospheric absorption/emission: not considered

**Total Type B uncertainty (RSS):**

	<b>B1</b>	<b>B2</b>	<b>B3</b>	<b>B4</b>	<b>B5</b>	<b>B6</b>	<b>Mean</b>
<b>K</b>	0.9	0.5	0.4	0.5	0.4	0.4	0.5

**Type A + Type B uncertainty (RSS): 0.5 K**

**Operational methodology during measurement campaign:** Calibration measurements were performed in the laboratory following, as close as possible, the procedures described in the Draft Protocol. The Landcal Blackbody Source P80P was set at four temperatures (278, 283, 293 and 303 K) in two different runs. Enough time was allowed for the blackbody to reach equilibrium at each temperature. Radiometer was aligned with the blackbody cavity, and placed at a distance so that the field of view was smaller than the cavity diameter. Standard processing (see references above) was applied to the radiometer readouts to calculate the equivalent brightness temperature. The six bands of the CE312-2 instrument were used.

**Radiometer usage (deployment), previous use of instrument and planned applications.** Field measurements (hand held and tripod mounted) of land and sea surface temperature/emissivity. Validation of thermal infrared images from satellite sensors in Canary Islands as well as laboratory measurements of soil and vegetation emissivity. Planned validation of thermal infrared images from cameras on board UAVs in forest and crops in Macaronesian region.

### 3.5.2 Uncertainty contributions associated with GOTA's measurements at NPL

<b>Uncertainty Contribution</b>	<b>Type A Uncertainty in Value / %</b>	<b>Type B Uncertainty in Value / (appropriate units)</b>	<b>Uncertainty in Brightness temperature K</b>
<b>Repeatability of measurement</b>	0.03%		0.09 K
<b>Reproducibility of measurement</b>	0.01%		0.03 K
<b>Primary calibration</b>		0.4 K	0.4 K
<b>Linearity of radiometer</b>		0.10 K	0.1 K
<b>Drift since calibration</b>		-	-
<b>Ambient temperature fluctuations</b>		0.3 K	0.3 K
<b>Size-of-Source Effect</b>		-	-
<b>Atmospheric absorption/emission</b>		-	-
<b>RMS total</b>	0.03% / 0.09 K	4 0.5 K	0.5 K

Mean values for six bands (B1 - B6) are shown. Values for each band are in section 3.10.1.



### 3.5.3 WST Measurements made by the GOTA CE312-2 radiometer

Figure 3.5.1 shows the output of the GOTA CE312-2 radiometer when it was viewing the surface of Wraysbury reservoir for the first two days of the five-day measurement campaign. The uncertainty bars (shown in black) represent the uncertainty values provided by GOTA which correspond to the measurements shown in the Figure. Figure 3.5.2 shows the plot of the difference of the measurements of the water surface temperature of Wraysbury reservoir made by the GOTA CE312-2 radiometer and the mean of all measurements, over the five-day measurement period.

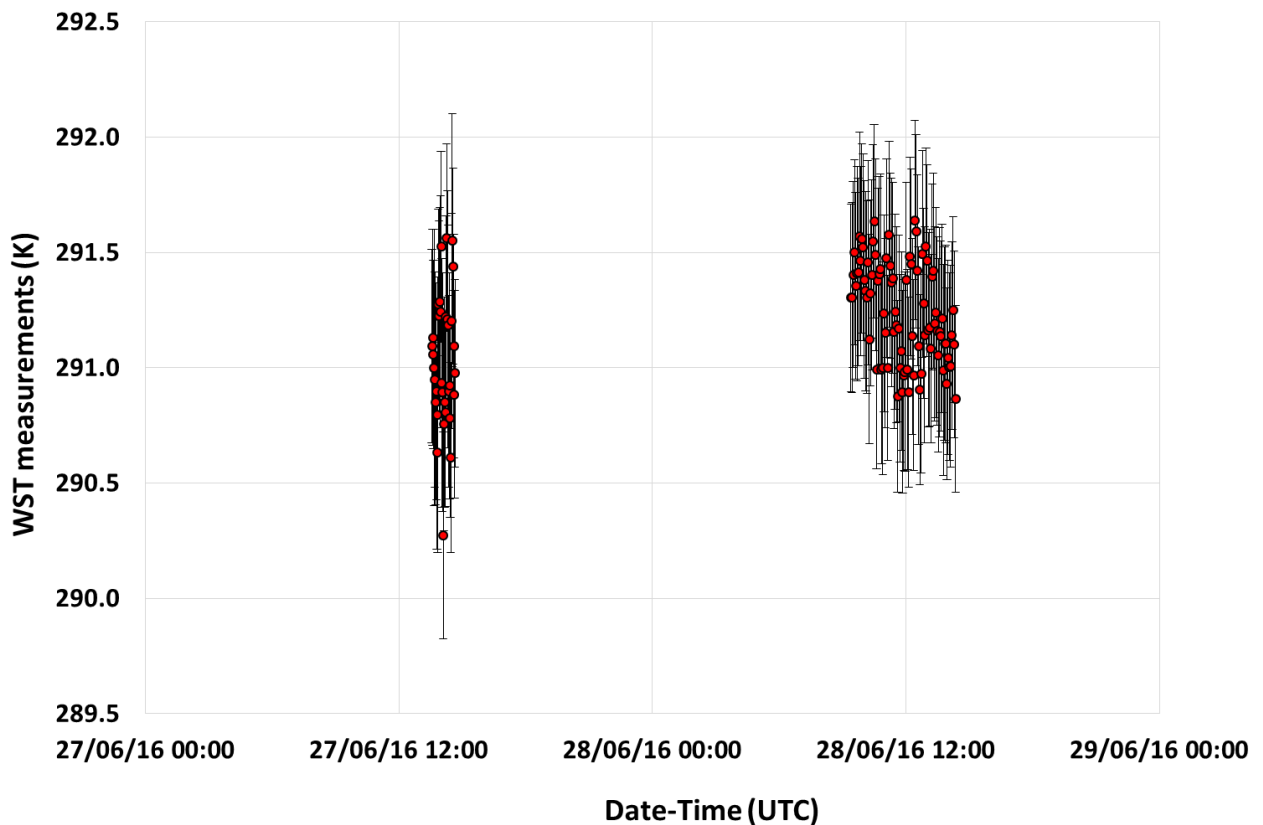


Figure 3.5.1: Measurements of the water surface temperature of Wraysbury reservoir made by the GOTA CE312-2 radiometer.

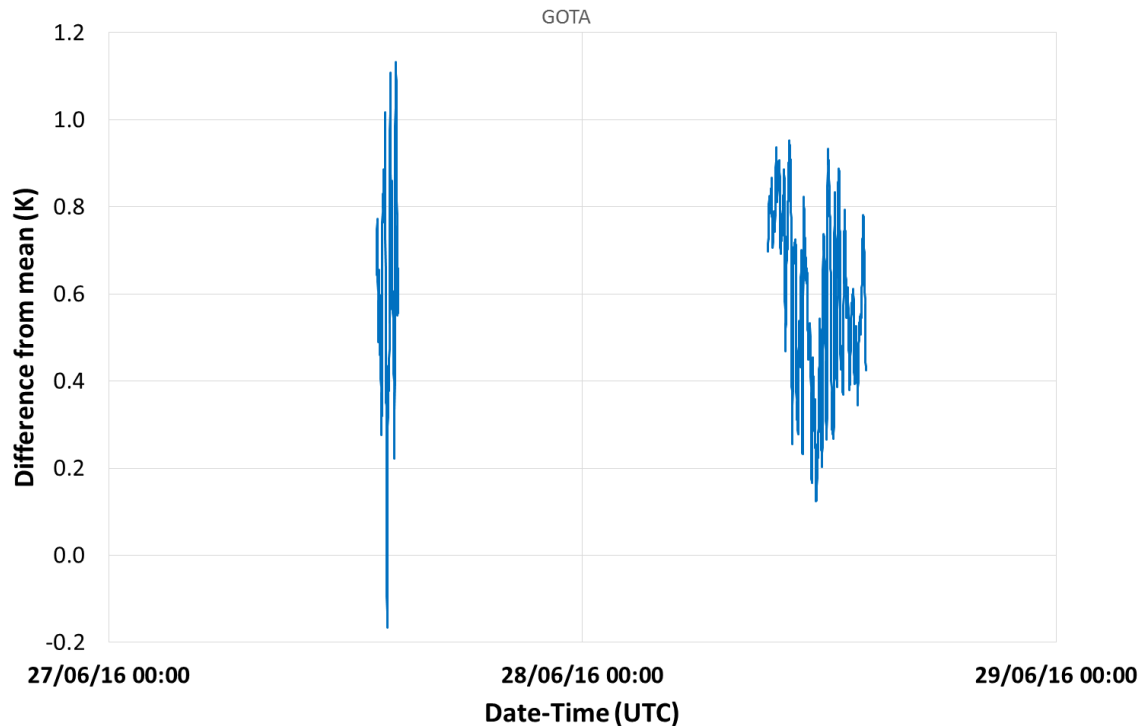


Figure 3.5.2: Difference of the WST of Wraysbury reservoir obtained by the GOTA CE312-2 radiometer and the mean of the WST provided by the 10 participants, over the five-day measurement period.

### 3.6 MEASUREMENTS MADE BY STFC RAL

Institute/organisation: Science and Technology Facilities Council Rutherford Appleton Laboratory  
 Chilton, Didcot, Oxon  
 OX11 0QX, United Kingdom  
 Contact Name: Tim Nightingale  
 Email: [Tim.Nightingale@stfc.ac.uk](mailto:Tim.Nightingale@stfc.ac.uk)

#### 3.6.1 Description of the radiometer and route of tracibility

##### Make and type of Radiometer:

Scanning Infrared Sea Surface Temperature Radiometer (SISTeR) manufactured by RAL Space.

##### Outline Technical description of instrument:

SISTeR is a chopped, self-calibrating filter radiometer manufactured by RAL Space. It has a single-element DLaTGS pyroelectric detector, a filter wheel containing up to six band-defining filters and two internal reference blackbodies, one operating at ambient temperature and the other heated to approximately 17 K above ambient. During operation the radiometer selects with a scan mirror successive views to each of the black bodies and to the external scene in a repeated sequence. For Sea Surface Temperature (SST) measurements, the external

measurements include views to the sea surface and to the sky at the complementary angle. The instrument field of view is approximately 13°. In this comparison, a filter centred at 10.8 µm was used.

**Reference:**

Further information on the SISTeR radiometer can be found in <http://www.stfc.ac.uk/research/environment/sister/>

**3.6.2 Establishment or traceability route for primary calibration including date of last realisation and breakdown of uncertainty:**

The primary traceability route is through two rhodium iron thermometers, one embedded in each of the instrument's internal blackbodies. These thermometers are re-calibrated periodically against a secondary SPRT in a dedicated thermal block maintained by Oxford University. The SPRT calibration is traceable to NPL. The estimated re-calibration accuracy is approximately 4 mK. The last calibration of the internal blackbody thermometers used in the FRM4STS measurements took place in 2007/2008 and new calibration is scheduled.

There is circumstantial evidence that the hot blackbody thermometer calibration may have shifted since its last re-calibration, by of order 50 mK. This will be confirmed by the next thermometer re-calibration.

The SISTeR calibration is validated against a CASOTS Mk 1 external black body, which is a copper cavity with Mankiewicz Nextel Velvet Coating 811-21, thermally controlled by a water bath. The temperature of the water bath is measured with a Fluke 5640 series thermistor probe, with a system accuracy of 4 mK, traceable to NIST.

A new calibrated thermistor probe and bridge was purchased in July 2016. When the two probes were inter-compared in the blackbody waterbath, their measurements agreed comfortably to within their estimated uncertainties.

**Radiometer usage (deployment), previous use of instrument and planned applications:**

The SISTeR radiometer was developed to collect SST validation data for the ATSR series of satellite radiometers. Latterly it supports the SLSTR and other satellite radiometers. The SISTeR instrument is currently deployed on the Queen Mary 2 cruise liner which is operated by Cunard Line. Deployments have been funded, at different times, by ESA, DECC and NERC. Typical routes are between Hamburg, Southampton and New York with side-trips from these ports, for example, to the Caribbean or to the Channel Islands. For four months of each year, from January to May, there is a round-the-world trip beginning and ending at Southampton.

**Uncertainty contributions associated with STFC RAL's measurements at NPL**

**Uncertainty breakdown:**

The uncertainties are given for both level 1 and level 3 data.

NPL lab measurements:

Level 1: Type A: 31 to 119 mK  
Type B: 12 to 128 mK

Level 3: Type A: 5 to 21 mK  
 Type B: 12 to 127 mK

Systematic inputs to the uncertainty model include the uncertainties on the instrument background radiance, the internal blackbody temperatures and emissivities, and the reflectance of the reservoir water surface.

Random inputs to the uncertainty model include the noise on measured thermometer counts, the noise on detector counts when viewing the internal blackbodies, and the variability of the measured sky radiances.

### 3.6.3 STFC RAL SISTeR measurements of Wraybury reservoir surface temperature

Figure 3.6.1 shows the measurements made by the STFC RAL SISTeR radiometer when it was viewing the surface of Wraybury reservoir over five days. The uncertainty bars (shown in brown) represent the uncertainty values provided by STFC RAL which correspond to the measurements shown in the Figure. Figure 3.6.2 shows the difference of the measurements of the water surface temperature of Wraybury reservoir made by the STFC RAL SISTeR radiometer and the mean of all measurements, over the five-day measurement period.

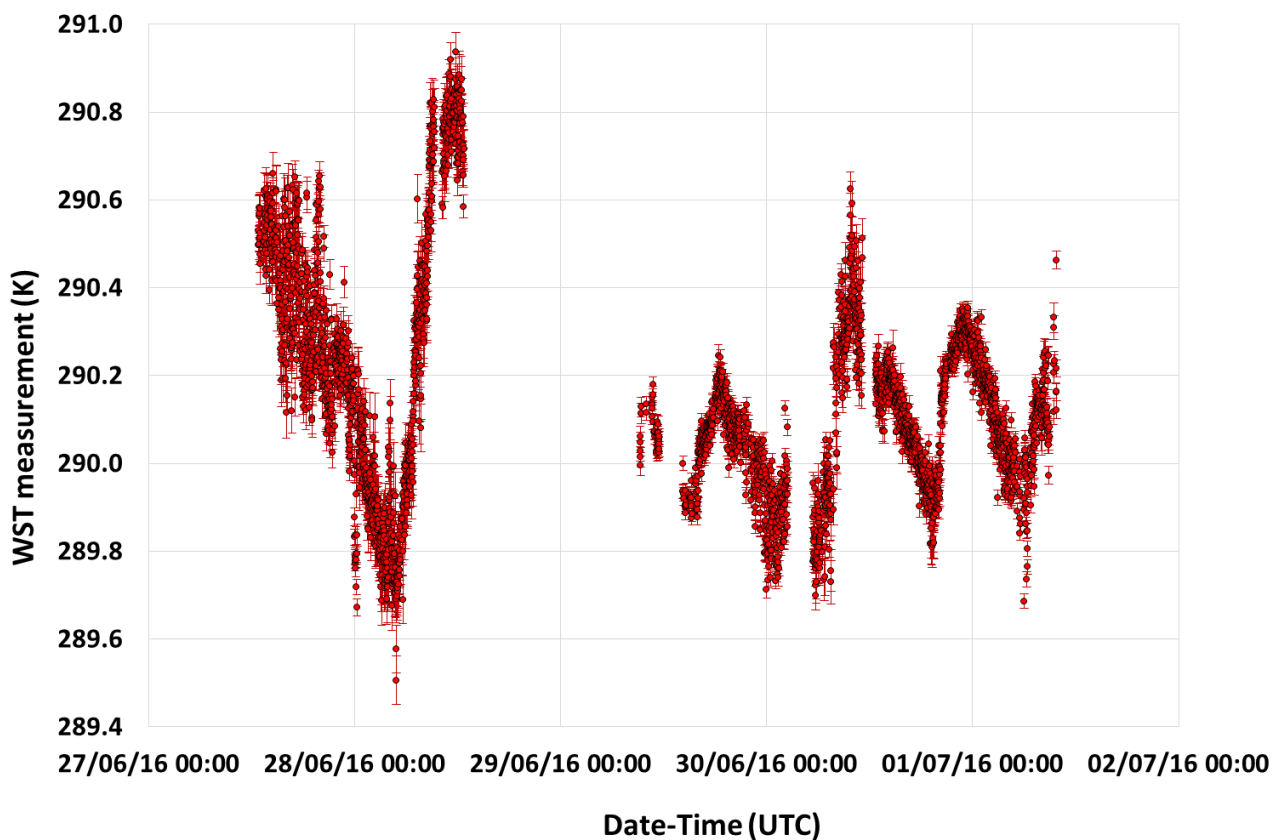


Figure 3.6.1: Measurements of the water surface temperature of Wraybury reservoir made by the STFC RAL SISTeR radiometer.

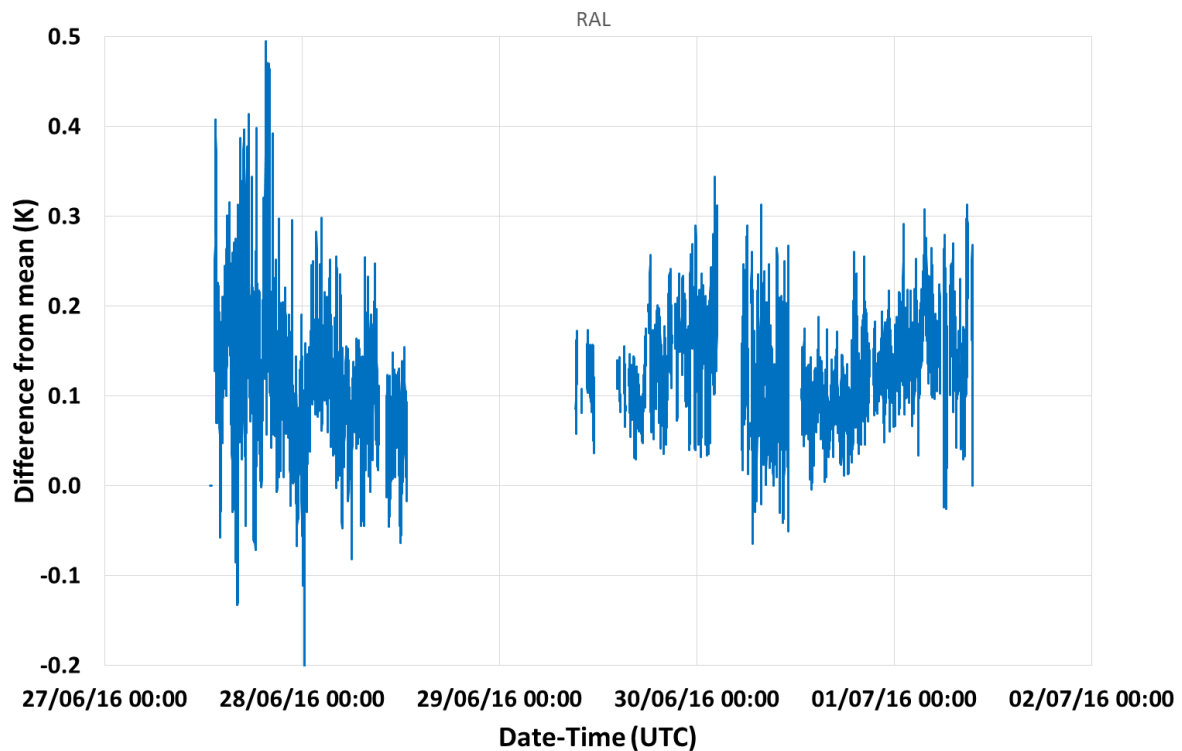


Figure 3.6.2: Difference of the WST of Wraysbury reservoir obtained by the STFC RAL SISTeR radiometer and the mean of the WST provided by the 10 participants, over the five-day measurement period.

### 3.7 MEASUREMENTS MADE BY SOUTHAMPTON UNIVERSITY

Institute/organisation: University of Southampton  
 Ocean and Earth Science, National Oceanography Centre Southampton  
 University of Southampton Waterfront Campus European Way Southampton  
 SO14 3ZH United Kingdom  
 Contact Name: Werenfrid Wimmer  
 Email: [w.wimmer@soton.ac.uk](mailto:w.wimmer@soton.ac.uk)

#### 3.7.1 Description of radiometer and route of traceability

Type: ISAR  
 Field of view: 3.5 degree half angle  
 Spectral band: 9.6-11.5 micrometer  
 Temperature resolution: 0.01 K  
 Uncertainty in measurements: 0.05 K + see paper (it's at least 0.05 as this is the uncertainty of the blackbody thermistors, but generally larger depending on emissivity and platform)

### 3.7.2 Uncertainty contributions associated with UoS measurements at NPL

Table 3.7.1 shows the uncertainty budget associated with measurements made by the Southampton University radiometer.

**Table 3.7.1: The uncertainty budget associated with measurements made by the Southampton University radiometer.**

e	Item	Uncertainty	Unit	Type
1	Detector linearity	<0.01 %	K month <sup>-1</sup>	B
2	Detector noise	~0.002	Volts	A
3	Detector accuracy	±0.5	K	B
4	ADC	±1(±76.3)	LSB (μV)	B
5	ADC accuracy	±0.1%	Range	B
6	ADC zero drift	±6	μV °C <sup>-1</sup>	B
7	Reference voltage 16-bit ADC	±15	mV	B
8	Reference voltage 12-bit ADC	±20	mV	B
9	Reference resistor	1	%	B
10	Reference resistor temperature coefficient	±100	Ppm °C <sup>-1</sup>	B
11	BB emissivity	±0.000178	Emissivity	B
12	Sea surface emissivity	±0.07	Emissivity	B
13	Steinhart–Hart approximation	±0.01	K	B
14	Radiate transfer approximation	±0.001	K	B
15	Thermistor	±0.05	K	B
16	Thermistor noise	~0.002	V	A

Sources of uncertainties arising within the ISAR SST retrieval processor. A more detailed breakdown is available in the reference paper below.

Reference: Wimmer, W., and I. Robinson, 2016: The ISAR instrument uncertainty model. *J. Atmos. Oceanic Technol.* doi:10.1175/JTECH-D-16-0096.1, in press.

### 3.7.3 UoS ISAR measurements of Wraysbury reservoir surface temperature

Figure 3.7.1 shows the output of the UoS ISAR radiometer when it was viewing the surface of Wraysbury reservoir over five days. The uncertainty bars (shown in brown) represent the uncertainty values provided by University of Southampton which correspond to the measurements shown in the Figure. Figure 3.7.2 shows the difference of the measurements of the water surface temperature of Wraysbury reservoir made by the UoS ISAR radiometer when it was viewing the surface of Wraysbury reservoir and the mean of all measurements, over the five-day measurement period.

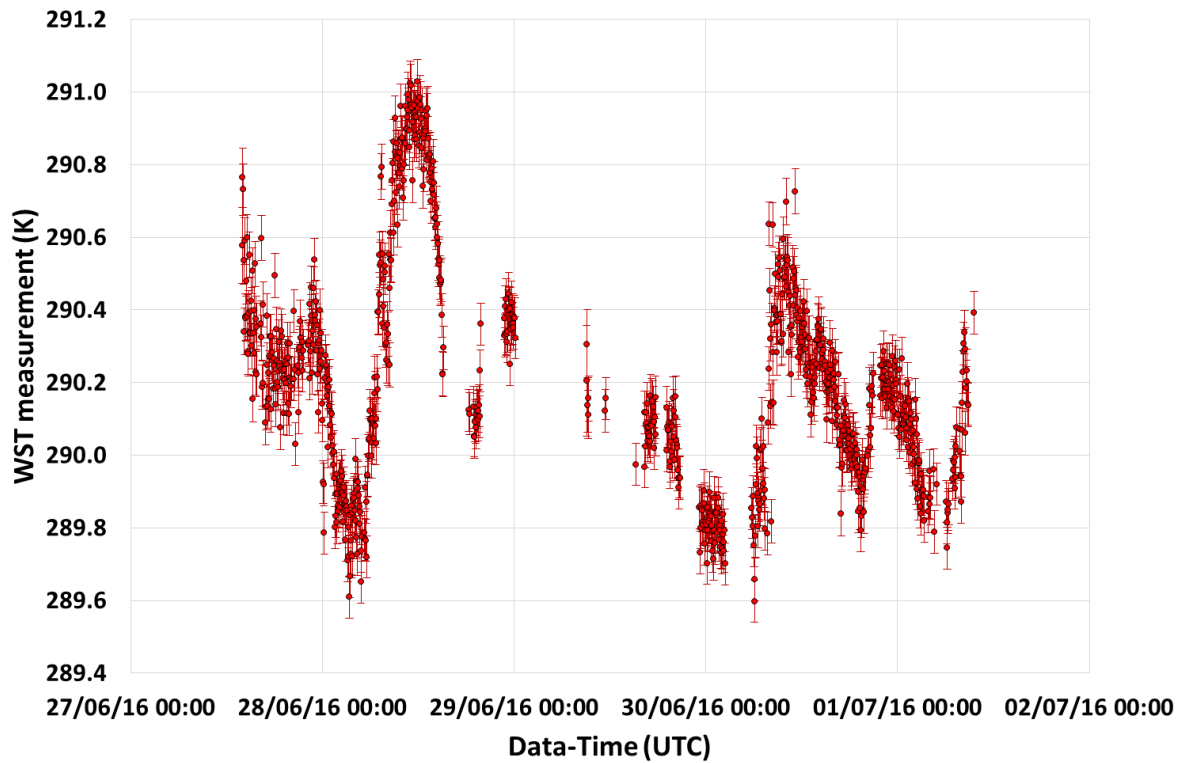


Figure 3.7.1: Measurements of the water surface temperature of Wraysbury reservoir made by the UoS ISAR radiometer.

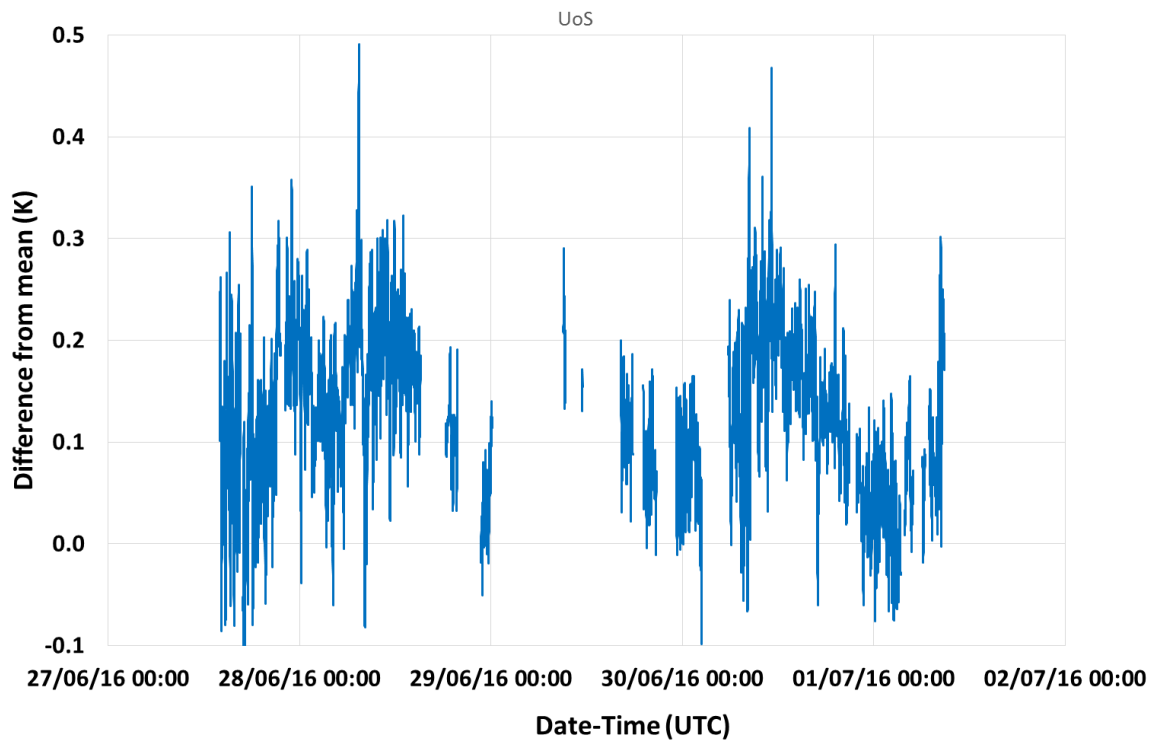


Figure 3.7.2: Difference of the WST of Wraysbury reservoir obtained by the UoS ISAR radiometer and the mean of the WST provided by the 10 participants, over the five-day measurement period.

### 3.8 MEASUREMENTS MADE BY DMI

Institute/organisation: Danish Meteorological Institute  
 Centre for Ocean and Ice, Lyngbyvej 100, 2100 København Ø  
 Contact Name: Jacob Høyer  
 Email: [jlh@dmu.dk](mailto:jlh@dmu.dk)

#### 3.8.1 Description of radiometers and route of traceability

##### **Make and type of Radiometer: ISAR**

The DMI TIR is an ISAR-5D, build by NOCS in 2012.

**Outline Technical description of instrument:** The radiometer is a self-calibrating radiometer, see: Donlon, C., Robinson, I. S., Wimmer, W., Fisher, G., Reynolds, M., Edwards, R., & Nightingale, T. J. (2008). An infrared sea surface temperature autonomous radiometer (ISAR) for deployment aboard volunteer observing ships (VOS). *Journal of Atmospheric and Oceanic Technology*, 25(1), 93-113.

**Establishment or traceability route for primary calibration including date of last realisation and breakdown of uncertainty:** The ISARS have been calibrated using the CASOTS blackbody, similar to the procedures used by Fred Wimmer, NOCS.

##### **Operational methodology during measurement campaign:**

The operational procedure for the DMI ISAR is to perform a calibration with the CASOTS blackbody, before and after any deployment over ice or water.

##### **Radiometer usage (deployment), previous use of instrument and planned applications.**

The DMI ISAR has been deployed at ships between Denmark and Greenland to observe SST. In addition, the DMI ISAR has participated in several field campaigns in the Arctic, to perform Ice surface temperature radiometer observations. The DMI ISAR has participated in the IST FICE campaign in March-April 2016.

#### 3.8.2 Uncertainty contributions associated with DMI's ISAR measurements at NPL

Table 3.8.1 shows the uncertainty budget associated with measurements made by the DMI radiometer.



**Table 3.8.1 shows the uncertainty budget associated with measurements made by the DMI radiometer**

e	Item	Uncertainty	Unit	Type
1	Detector linearity	<0.01 %	K month <sup>-1</sup>	B
2	Detector noise	~0.002	Volts	A
3	Detector accuracy	±0.5	K	B
4	ADC	±1(±76.3)	LSB (μV)	B
5	ADC accuracy	±0.1%	Range	B
6	ADC zero drift	±6	μV °C <sup>-1</sup>	B
7	Reference voltage 16-bit ADC	±15	mV	B
8	Reference voltage 12-bit ADC	±20	mV	B
9	Reference resistor	1	%	B
10	Reference resistor temperature coefficient	±100	Ppm °C <sup>-1</sup>	B
11	BB emissivity	±0.000178	Emissivity	B
12	Sea surface emissivity	±0.07	Emissivity	B
13	Steinhart–Hart approximation	±0.01	K	B
14	Radiate transfer approximation	±0.001	K	B
15	Thermistor	±0.05	K	B
16	Thermistor noise	~0.002	V	A

Sources of uncertainties arising within the ISAR SST retrieval processor. A more detailed breakdown is available in the reference paper: Wimmer, W., and I. Robinson, 2016: The ISAR instrument uncertainty model. *J. Atmos. Oceanic Technol.* doi:10.1175/JTECH-D-16-0096.1, in press.

### 3.8.3 DMI ISAR radiometer WST measurements of Wraysbury reservoir

Figure 3.8.1 shows the output of the DMI ISAR radiometer when it was viewing the surface of Wraysbury reservoir over five days. The uncertainty bars (shown in brown) represent the uncertainty values provided by DMI which correspond to the measurements shown in the Figure. Figure 3.8.2 shows the difference of the measurements of the water surface temperature of Wraysbury reservoir made by the DMI ISAR radiometer when it was viewing the surface of Wraysbury reservoir and the mean of all measurements, over the five-day measurement period.

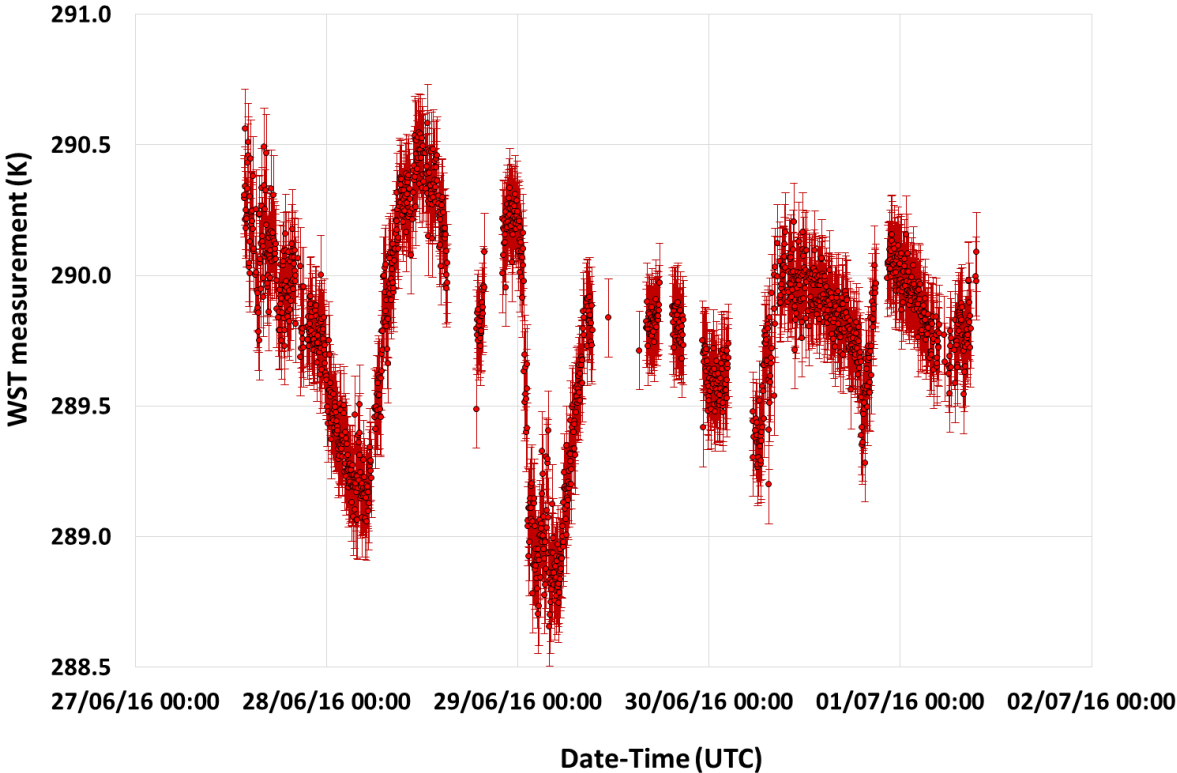


Figure 3.8.1: Measurements of the water surface temperature of Wraysbury reservoir made by the DMI ISAR radiometer.

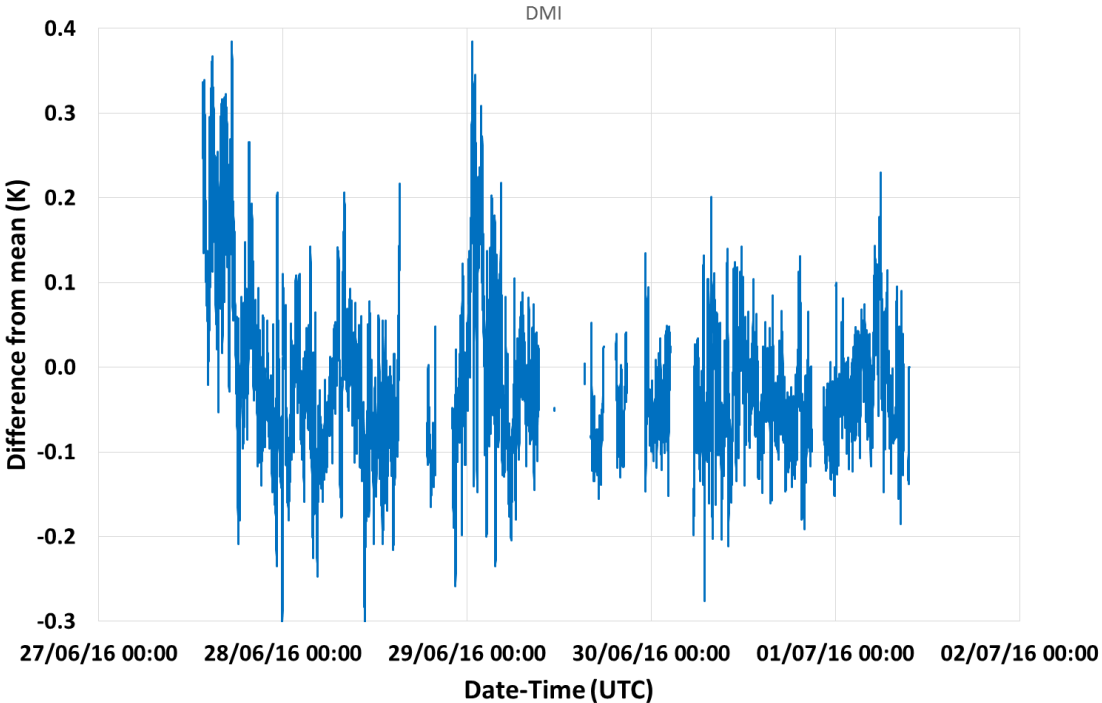


Figure 3.8.2: Difference of the WST of Wraysbury reservoir obtained by the DMI ISAR radiometer and the mean of the WST provided by the 10 participants, over the five-day measurement period.

### 3.8.4 Additional comments from institute

#### Information about the WST experiment data acquired by the DMI ISAR

The reference thermistors which measure the temperature of the blackbodies within ISAR looked stable, so DMI have processed the data in the normal way, but they still are not confident that the ISAR observations are OK. Additional comments can be found in section 3.8.4 in the corresponding NPL radiometer report (Barker Snook et al, 2017) as part of the 2016 FRM4STS intercomparison.

### 3.9 MEASUREMENTS MADE BY OUC, QINGDAO

Institute/organisation: Ocean University of China  
238 Songling Road, Qingdao, 266100, China  
Contact Name: Kailin Zhang  
Email: [zhangkl@ouc.edu.cn](mailto:zhangkl@ouc.edu.cn)

#### 3.9.1 Description of radiometers and route of traceability

##### 3.9.1.1 Radiometer ISAR

###### Make and type of Radiometer

Infrared Sea Surface Temperature Autonomous Radiometer (ISAR)

###### Outline Technical description of instrument:

Detector: Heitronics KT15.85 IIP 8115, Spectral bands: 9.6-11.5 $\mu$ m, Calibration type: 2 internal blackbody cavities. For full information see: Donlon, C. J., I. S. Robinson, M. Reynolds, W. Wimmer, G. Fisher, R. Edwards, and T. J. Nightingale, 2008: "An Infrared Sea Surface Temperature Autonomous Radiometer (ISAR) for Deployment aboard Volunteer Observing Ships (VOS)", *J. Atmos. Oceanic Technol.*, **25**, 93-113.

###### Establishment or traceability route for primary calibration including date of last realisation and breakdown of uncertainty:

ISAR has undergone primary calibration by the manufacturer. Re-calibrations are performed before and after each measurement campaign using the blackbody manufactured by LR TECH INC. The overall uncertainty of ISAR is about 0.1 K. (Wimmer, W., and I. Robinson, 2016: The ISAR instrument uncertainty model. *J. Atmos. Oceanic Technol.* doi:10.1175/JTECH-D-16-0096.1, in press).

###### Operational methodology during measurement campaign:

ISAR measures both the sea surface radiance and the down-welling atmosphere radiance which are calibrated by two reference blackbody cavities. During one measuring cycle, ISAR measures the ambient blackbody 30 times, the heated blackbody 30 times, the sky 10 times and the sea surface 40 times. Using the self-calibration system in ISAR, SST is calculated for each measuring cycle. (Donlon, C. J., I. S. Robinson, M. Reynolds, W. Wimmer, G. Fisher, R. Edwards, and T. J. Nightingale, 2008: An Infrared Sea Surface Temperature Autonomous Radiometer (ISAR) for Deployment aboard Volunteer Observing Ships (VOS), *J. Atmos. Oceanic Technol.*, **25**, 93-113)

**Radiometer usage (deployment), previous use of instrument and planned applications.**

The ISAR has been deployed on the research vessel Dong Fang Hong II of Ocean University of China and continuously operating mainly in the China Seas since 2009.

**3.9.1.2 Radiometer OUCFIRST****Make and type of Radiometer**

Ocean University of China First Infrared Radiometer for measurements of Sea Surface Temperature (OUCFIRST)

**Outline Technical description of instrument:**

Detector: Heitronics KT15.85 IIP 9928, Spectral bands: 9.6-11.5 $\mu$ m, Calibration type: two internal blackbodies.

**Establishment or traceability route for primary calibration including date of last realisation and breakdown of uncertainty:**

OUCFIRST is calibrated before and after each measurement campaign using the blackbody manufactured by LR TECH INC. The overall uncertainty of OUCFIRST is about 0.1 K.

**Operational methodology during measurement campaign:**

OUCFIRST has two measurement modes, one for lab calibration and the other one for outdoor measurement. For lab calibration, OUCFIRST measures the ambient blackbody 30 times, the heated blackbody 30 times and target blackbody 40 times. For outdoor mode, OUCFIRST measures the ambient blackbody 30 times, the heated blackbody 30 times, the sky 10 times and the sea 40 times. Using the self-calibration system in OUCFIRST, SST is calculated for each measuring cycle.

**Radiometer usage (deployment), previous use of instrument and planned applications.**

OUCFIRST is now under testing and has been deployed on the research vessel Dong Fang Hong II of the Ocean University of China and operated for three campaigns in the China Seas in 2015 and 2016.

**3.9.2 Uncertainty contributions associated with OUC's measurements at NPL****3.9.2.1 Uncertainty contributions of measurements by ISAR**

Table 3.9.2.1 shows the uncertainty budget associated with measurements made by the OUC radiometer.

**Table 3.9.2.1: The uncertainty budget associated with measurements made by the OUC radiometer**

e	Item	Uncertainty	Unit	Type
1	Detector linearity	<0.01 %	K month <sup>-1</sup>	B
2	Detector noise	~0.002	Volts	A
3	Detector accuracy	±0.5	K	B
4	ADC	±1(±76.3)	LSB (μV)	B
5	ADC accuracy	±0.1%	Range	B
6	ADC zero drift	±6	μV °C <sup>-1</sup>	B
7	Reference voltage 16-bit ADC	±15	mV	B
8	Reference voltage 12-bit ADC	±20	mV	B
9	Reference resistor	1	%	B
10	Reference resistor temperature coefficient	±100	Ppm °C <sup>-1</sup>	B
11	BB emissivity	±0.000178	Emissivity	B
12	Sea surface emissivity	±0.07	Emissivity	B
13	Steinhart–Hart approximation	±0.01	K	B
14	Radiate transfer approximation	±0.001	K	B
15	Thermistor	±0.05	K	B
16	Thermistor noise	~0.002	V	A

Sources of uncertainties arising within the ISAR SST retrieval processor. A more detailed breakdown is available in the reference paper: Wimmer, W., and I. Robinson, 2016: The ISAR instrument uncertainty model. *J. Atmos. Oceanic Technol.* doi:10.1175/JTECH-D-16-0096.1, in press.

### 3.9.2.2 Uncertainty contributions of measurements by OUCFIRST radiometer

Table 3.9.2.1 shows the uncertainty budget associated with measurements made by the OUC radiometer

**Table 3.9.2.2: The uncertainty budget associated with measurements made by the OUCFIRST radiometer**

Uncertainty Contribution	Type A Uncertainty in Value / %	Type B Uncertainty in Value	Uncertainty in Brightness temperature K
<b>Repeatability of measurement<sup>(1)</sup></b>	0.023 K /0.008%		0.023 K
<b>Reproducibility of measurement<sup>(2)</sup></b>	0.009 K /0.003%		0.009 K
<b>Primary calibration<sup>(3)</sup></b>		0.12 K	0.12 K
<b>RMS total</b>	0.025 K /0.008%	0.12 K	0.12 K

(1) Typical value of the standard deviation of 143 measurements at fixed black body temperature without re-alignment of radiometer.

(2) Typical value of difference between two runs of radiometer measurements at the same black body temperature including re-alignment.

(3) Typical value of difference between radiometer brightness temperature and ASSIST II Blackbody temperature.

### 3.9.3 OUC's radiometer measurements of the WST at Wraysbury reservoir.

#### 3.9.3.1 OUC ISAR radiometer measurements of the WST at Wraysbury reservoir

Figure 3.9.1 plots the measurements of the OUC ISAR radiometer when it was viewing the surface of the water at Wraysbury reservoir over five days. The uncertainty bars (shown in black) represent the uncertainty values provided by OUC which correspond to the measurements shown in the Figure. Figure 3.9.2 shows the difference of the measurements of the water surface temperature of Wraysbury reservoir made by the OUC ISAR radiometer when it was viewing the surface of Wraysbury reservoir and the mean of all measurements, over the five-day measurement period.

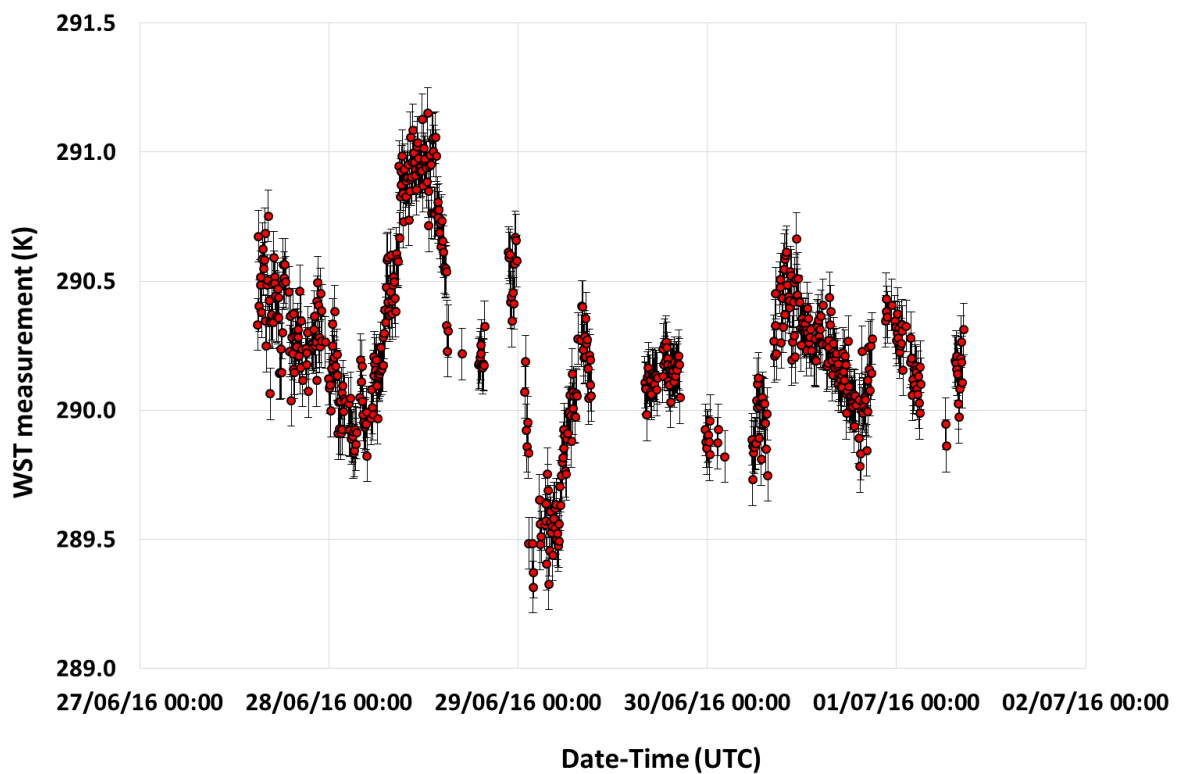


Figure 3.9.1: Measurements of the water surface temperature of Wraysbury reservoir made by the OUC ISAR radiometer.

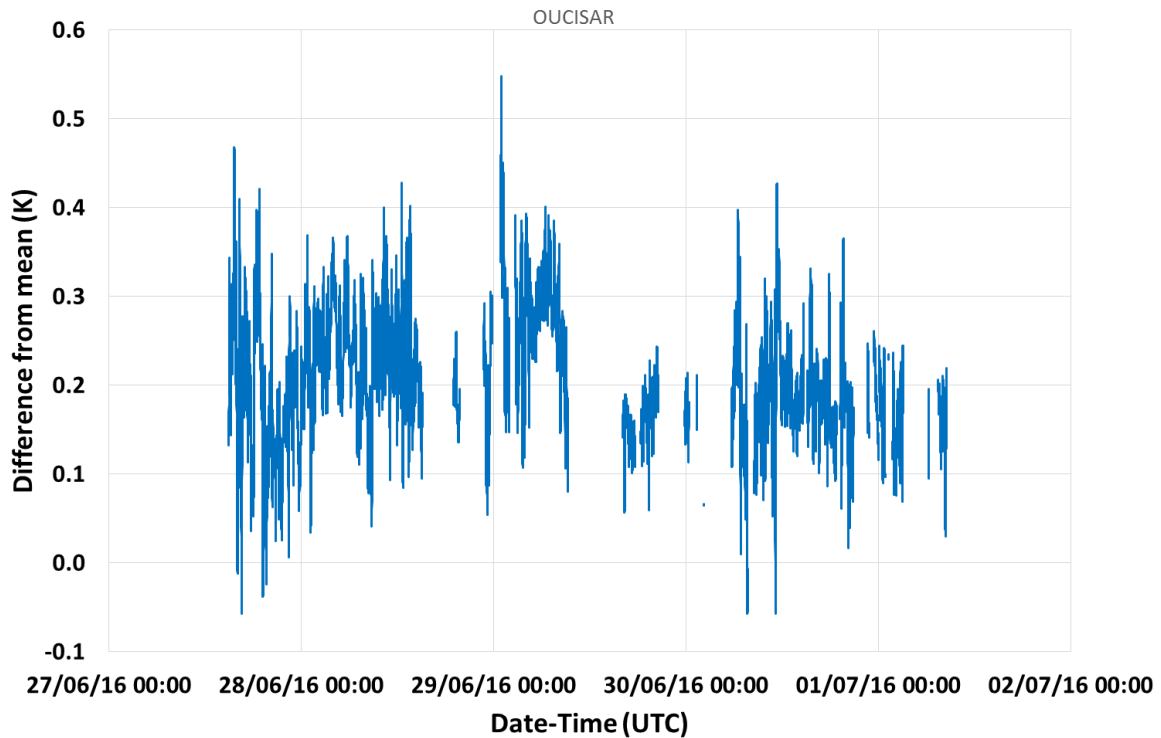


Figure 3.9.2: Difference of the measurements of the WST of Wraysbury reservoir made by the OUC ISAR radiometer from the mean of all measurements over the five-day measurement period.

### 3.9.3.2 OUCFIRST radiometer WST measurements at Wraysbury reservoir

Figure 3.9.3 shows the output of the OUCFIRST radiometer when it was viewing the surface of Wraysbury reservoir over five days. The uncertainty bars (shown in black) represent the uncertainty values provided by OUC which correspond to the measurements made by the OUCFIRST radiometer. Figure 3.9.4 shows the difference of the measurements of the WST of Wraysbury reservoir made by the OUCFIRST radiometer and the mean of all measurements over the five-day measurement period.

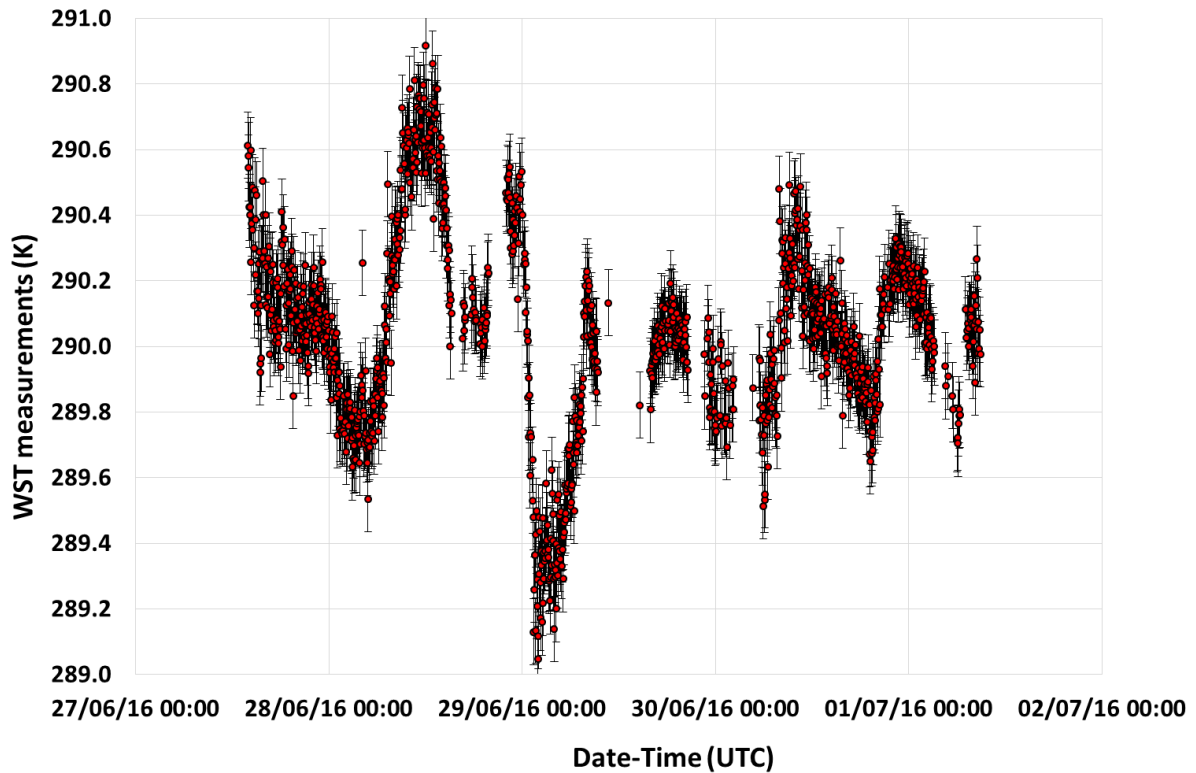


Figure 3.9.3: Measurements of the water surface temperature of Wraysbury reservoir made by the OUCFIRST radiometer.

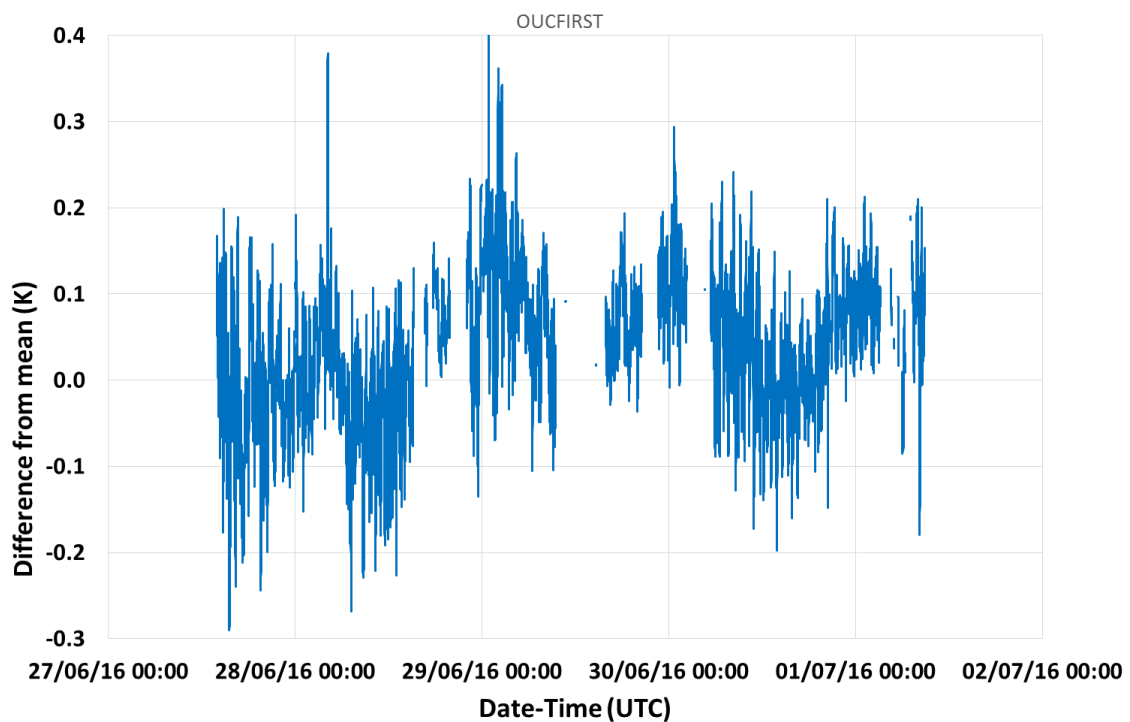


Figure 3.9.4: Difference of the measurements of the WST of Wraysbury reservoir made by the OUCFIRST radiometer and the mean of all measurements made over the five day period.



#### 4 SUMMARY OF THE RESULTS

This section provides a comparison of the water surface temperatures (WST) provided by the participants for Wraysbury reservoir during the week beginning on the 27<sup>th</sup> June 2016. A total of ten radiometers participated in the WST comparison and the participants provided their results at different times and at different temporal resolutions. In order to be able to compare their WSTs, a standard interpolation method was used to estimate the WST of the participants at the same 10 second time intervals.

WST measurements should ideally be compared to a mean, determined from the WST obtained with the different radiometers, weighted by their uncertainties. However, to do this requires a full breakdown of uncertainties so that the weights can be fully evaluated and agreed upon by participants in advance. This was not possible from the data provided by some participants. An alternative approach was adopted which uses the simple mean of the radiometer measurements. In reviewing the data, no consideration was also made as to potential differences between night-time and day-time measurements.

Figure 4.1 shows a plot of the WST measurements provided by the ten participating radiometers during the five-day comparison period. Each vertical gridline is plotted at midnight and represents the beginning of a new day of measurements. During the five-day measurement period, the WST varied over a range of about 2 K. The WST provided by the participants generally follow the same trend and there are relatively small biases between them. Figure 4.2 shows a similar plot to that of Figure 4.1 but leaves out the data provided by JPL and GOTA, which allows the temperature axis to be expanded.

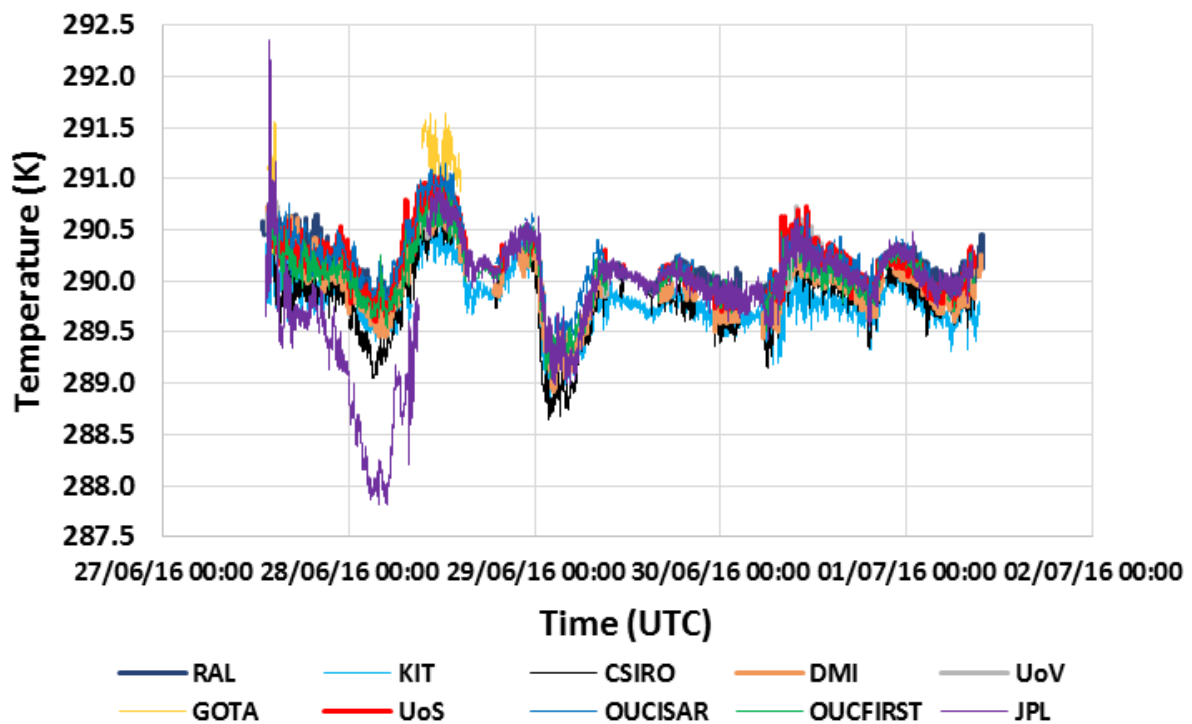


Figure 4.1: Plot of the WST measurements provided by the participants during the five-day comparison period. Each vertical gridline is plotted at midnight and represents the beginning of a new day of measurements.

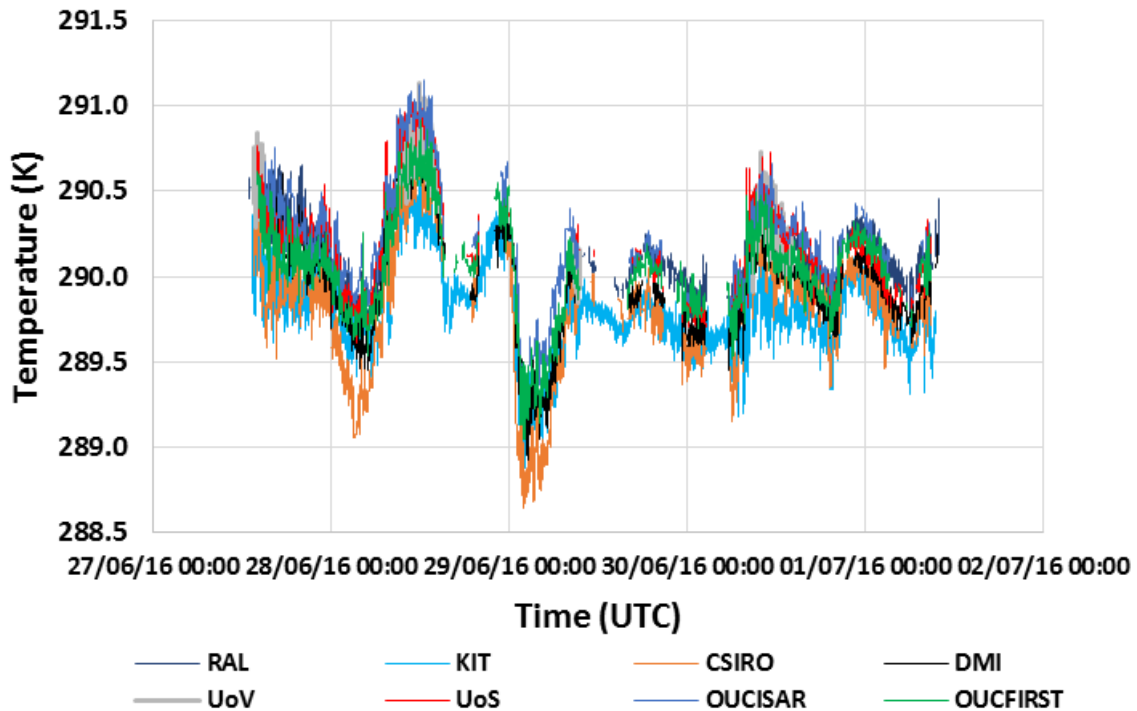


Figure 4.2: Plot of the WST measurements of the various participants, excluding JPL and GOTA, over the five-day comparison period.

Figure 4.3 shows a plot of the difference of the WST measurements of the various participants from their arithmetic mean, over the five-day comparison period. Because of biases in some of the measurements made by JPL and GOTA, the arithmetic mean used in these calculations did not include measurements made by these two participants. Each vertical gridline is plotted at midnight and represents the beginning of a new day of measurements. Plotting the measurements in this configuration highlights the biases which exist between the WST measurements acquired by the different participants. Figure 4.4 shows a similar plot to that shown in Figure 4.3 but leaves out the results for JPL and GOTA, which allows the temperature difference axis to be expanded. Figure 4.4 indicates that the bulk of the measurements made by eight of the participants appear to stay within a  $\pm 0.4$  K range of their arithmetic mean, throughout the five day measurement period. Finally, Figure 4.5 shows the corresponding plot with only the differences of the SST-measuring radiometers included (measurements of the LST-measuring radiometers have been excluded).

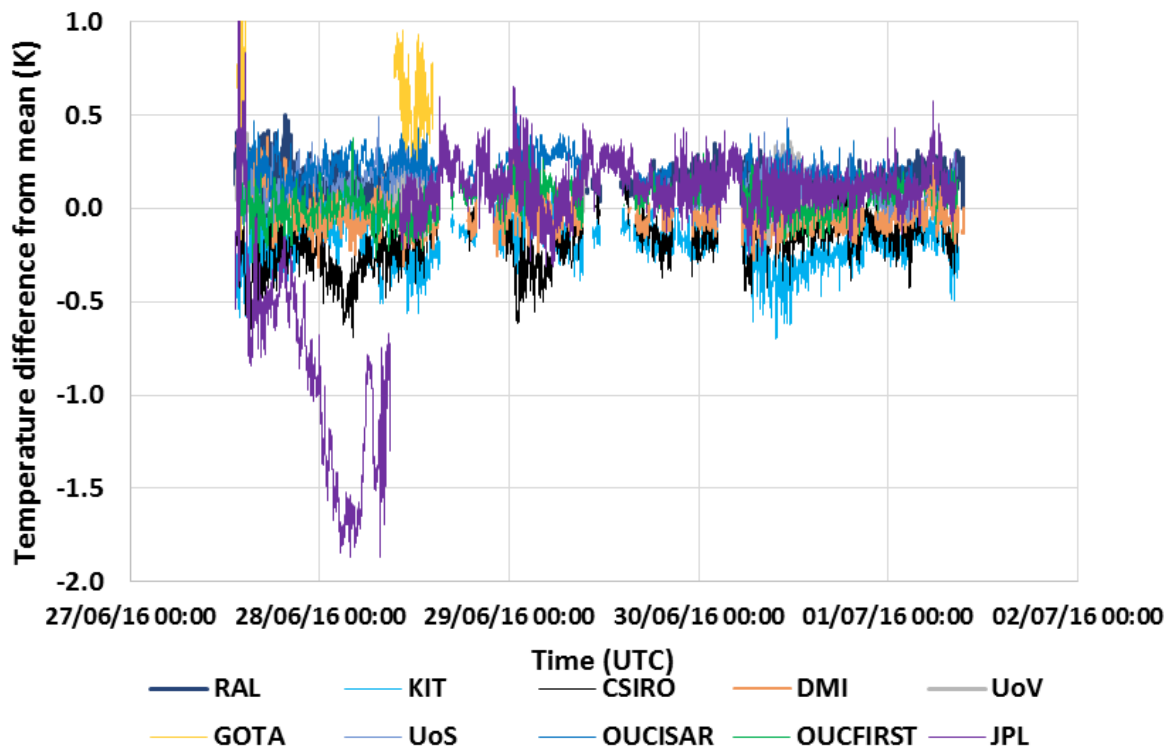


Figure 4.3: Plot of the difference of the WST measurements of the various participants from their arithmetic mean, over the five-day comparison period. Each vertical gridline is plotted at midnight and represents the beginning of a new day of measurements.

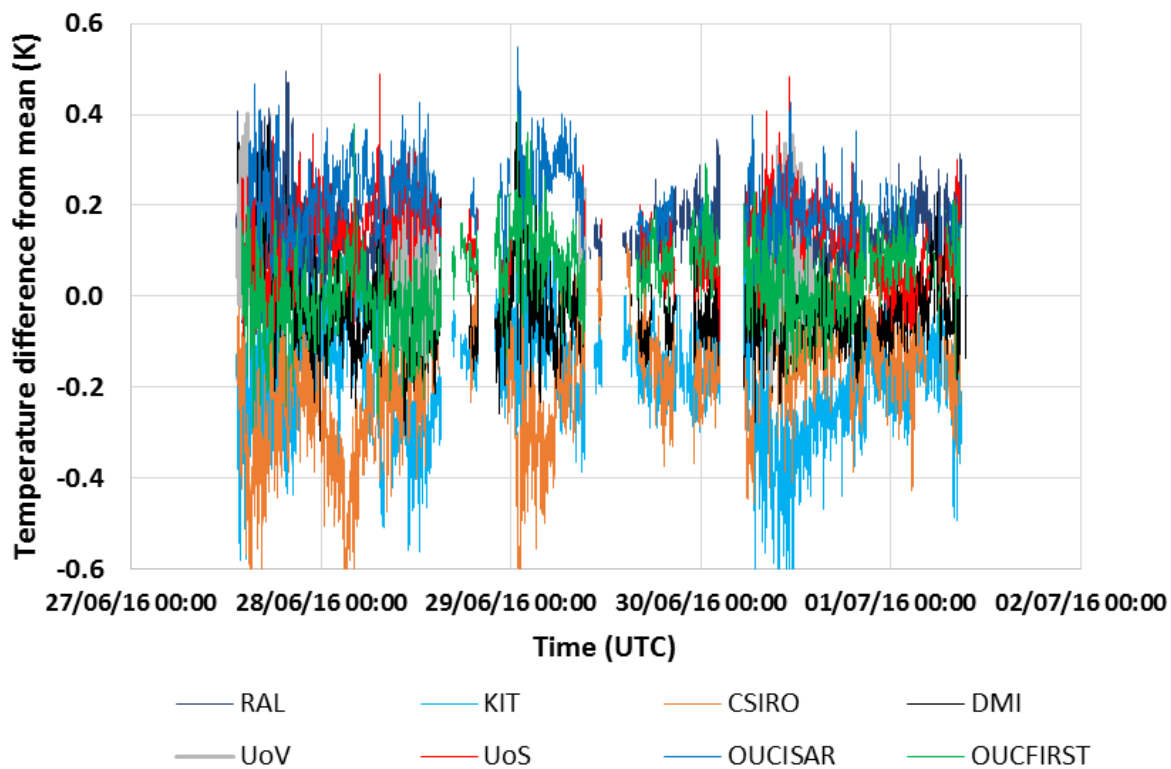


Figure 4.4: Plot of the difference of the WST measurements of the various participants from their arithmetic mean, excluding JPL and GOTA, over the five-day comparison period.

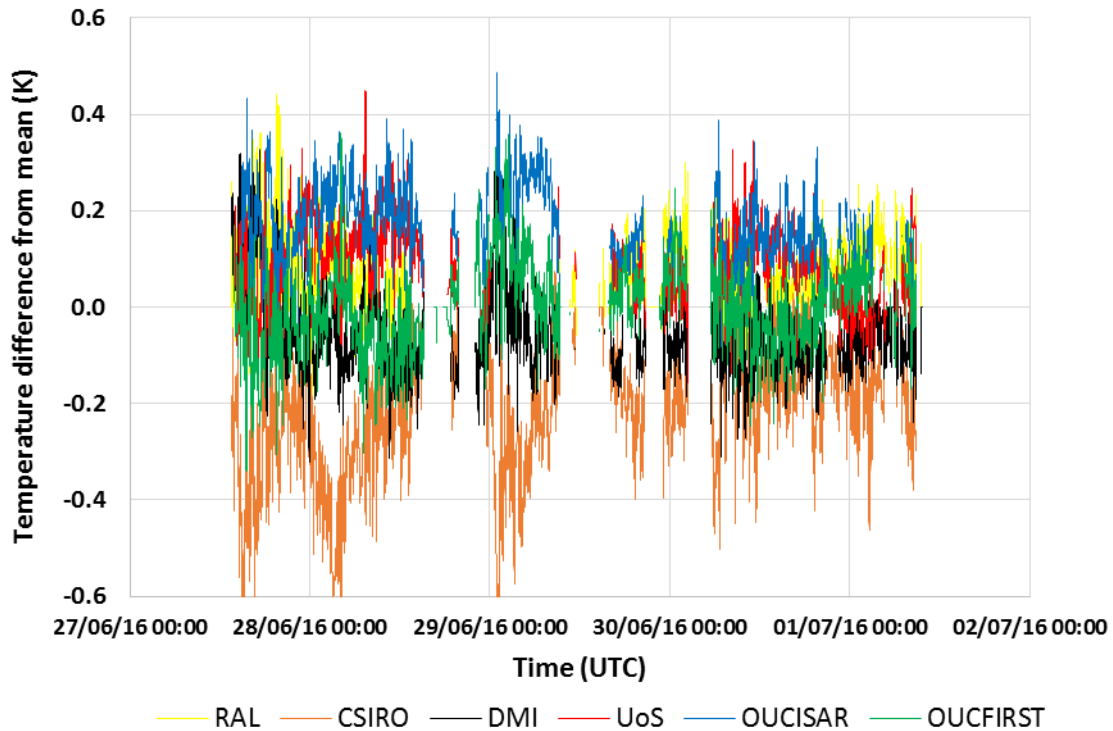


Figure 4.5: Plot of the difference of the WST measurements of the participating SST-measuring radiometers from their arithmetic mean, over the five-day comparison period.

Table 4.1 shows the difference between the mean of the average of the 10 radiometers who participated in the WST comparison over the five-day measurement period from the mean of the measurements of each radiometer over the same five day period. Note that only times when a particular radiometer was providing measurements were used to determine the mean of the average of the 10 radiometers. Note also that the measurements provided by JPL and GOTA were not used in the calculation of the mean.

Table 4.1: Difference of the mean of the average of the 10 radiometers who participated in the WST comparison averaged over the five-day measurement period from the mean of the measurements of each radiometer averaged over the same five day period.

<b>Radiometer</b>	<b>Mean difference from the mean (°C)</b>
<b>STFC RAL</b>	<b>0.123</b>
<b>KIT</b>	<b>-0.159</b>
<b>CSIRO</b>	<b>-0.189</b>
<b>DMI</b>	<b>-0.020</b>
<b>UoV</b>	<b>0.117</b>
<b>UoS</b>	<b>0.125</b>
<b>OUCFIRST</b>	<b>0.033</b>
<b>OUC-ISAR</b>	<b>0.206</b>
<b>GOTA</b>	<b>0.593</b>
<b>JPL</b>	<b>-0.109</b>

Table 4.2 shows the difference between the mean of the average of the 10 radiometers who participated in the WST comparison over the night-time of the five-day measurement period and the mean of the night-time measurements of each radiometer over the same five day period. Night-time measurements were taken as measurements between 19.00 at night and 6.00 (UTC) the following morning. Note that only times when a particular radiometer was providing measurements were used to determine the mean of the average of the 10 radiometers. Note that the measurements provided by JPL and GOTA were not used in the calculation of the mean. Finally, the UoV and GOTA radiometers were manually operated and did not provide any measurements during the night-time periods.

Table 4.2: Difference of the mean of the average of the 10 radiometers who participated in the WST comparison averaged over the night-time of the five-day measurement period from the mean of the night-time measurements of each radiometer averaged over the same five-day period.

<b>Radiometer</b>	<b>Mean difference from the mean (°C)</b>
<b>STFC RAL</b>	<b>0.136</b>
<b>KIT</b>	<b>-0.114</b>
<b>CSIRO</b>	<b>-0.224</b>
<b>DMI</b>	<b>-0.025</b>
<b>UoV</b>	
<b>UoS</b>	<b>0.096</b>
<b>OUCFIRST</b>	<b>0.065</b>
<b>OUC-ISAR</b>	<b>0.206</b>
<b>GOTA</b>	
<b>JPL</b>	<b>-0.189</b>

Table 4.3 shows the difference between the mean of the average of the 10 radiometers who participated in the WST comparison over the day-time of the five-day measurement period and the mean of the day-time measurements of each radiometer over the same five day period. Day-time measurements were taken as measurements between 6.00 and 19.00 (UTC) for each day of measurements. Note that only times when a particular radiometer was providing measurements were used to determine the mean of the average of the 10 radiometers. Note that the measurements provided by JPL and GOTA were not used in the calculation of the mean.

Table 4.3: Difference of the mean of the average of the 10 radiometers who participated in the WST comparison averaged over the day-time of the five-day measurement period from the mean of the day-time measurements of each radiometer averaged over the same five-day period.

<b>Radiometer</b>	<b>Mean difference from the mean (°C)</b>
<b>STFC RAL</b>	<b>0.111</b>
<b>KIT</b>	<b>-0.200</b>
<b>CSIRO</b>	<b>-0.164</b>
<b>DMI</b>	<b>-0.014</b>
<b>UoV</b>	<b>0.117</b>
<b>UoS</b>	<b>0.148</b>
<b>OUCFIRST</b>	<b>0.004</b>
<b>OUC-ISAR</b>	<b>0.206</b>
<b>GOTA</b>	<b>0.593</b>
<b>JPL</b>	<b>-0.032</b>

## **5 DISCUSSION**

### **5.1 RADIOMETER POSITIONING AT TEST SITE**

Concerns were raised about the positioning of the radiometers at Wraysbury reservoir. Due to the layout of the research raft on Wraysbury reservoir, it was decided that, in order for all radiometers to be viewing similar areas of the water surface, the radiometers should be positioned side-by-side on the eastern side of the platform. This raised the issue of shadows being introduced in the viewing areas of radiometers and potentially affecting the overall comparative results. However, measurements were taken during a summer month when the sun was high in the sky so the issue of shadows did not appear to affect the measurements during WST measurement campaign. However, it is recommended that care should be taken in future comparisons to ensure that radiometers are facing south in order to eliminate the issue of shadows wherever possible. This may mean opting for a more suitable testing facility or spending further time adapting and improving our current resources.

### **5.2 WEATHER AND AUTOMATION DURING CAMPAIGN**

While some instruments (e.g. ISAR) were fully automated to measure without supervision, a couple of institutes were unable to leave their instruments measuring overnight for fear of water damage. This meant that those institutes could only take measurements during the daylight hours and would have to start dismantling their set up at the first signs of rain. This is mostly due to the original use of the radiometers. Simple solutions could be performed to alleviate some of the hassle that comes with non-waterproof equipment as many institutes stored their electrics in pelicans or wrapped them in plastic bags for the duration of the comparison. For future comparison campaigns, more thought should be given to adverse weather conditions to utilise available resources as much as possible.

### 5.3 THE EFFECT OF THE WIND

The wind was monitored during the entire five day campaign in order to try and identify any correlation between wind speed and WST. Figure 5.1 shows the wind 2-D horizontal wind magnitude over the period of the comparison, provided by Southampton University. Comparison of Figure 5.1 with Figure 4.2 (the measurements of WST made by different participants) indicates that there is no significant correlation between wind magnitude and measured values of WST.

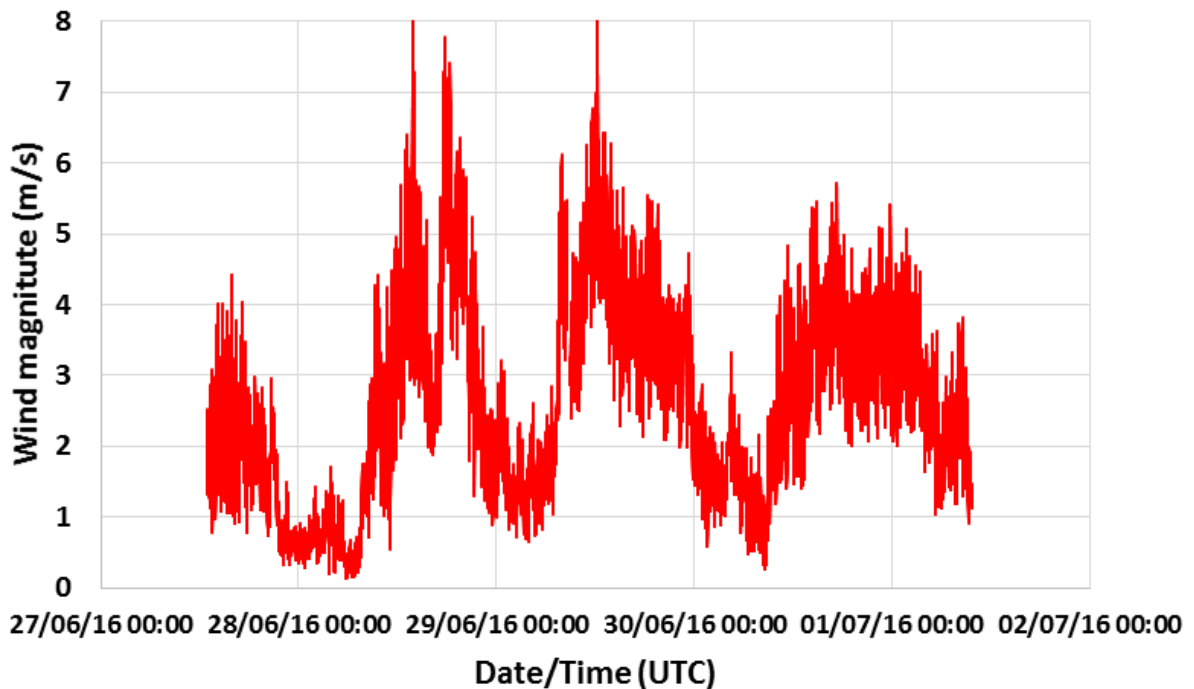


Figure 5.1: The 2-D horizontal wind magnitude plotted over the five-day period of the WST comparison (data provided by Southampton University).

Figure 5.2 shows a plot of the wind direction measured during the five day period of the comparison (data provided by Southampton University). Comparison of Figure 5.2 with Figure 4.2 (the measurements of WST made by different participants) indicates that there is no significant correlation between wind direction and measured values of WST.

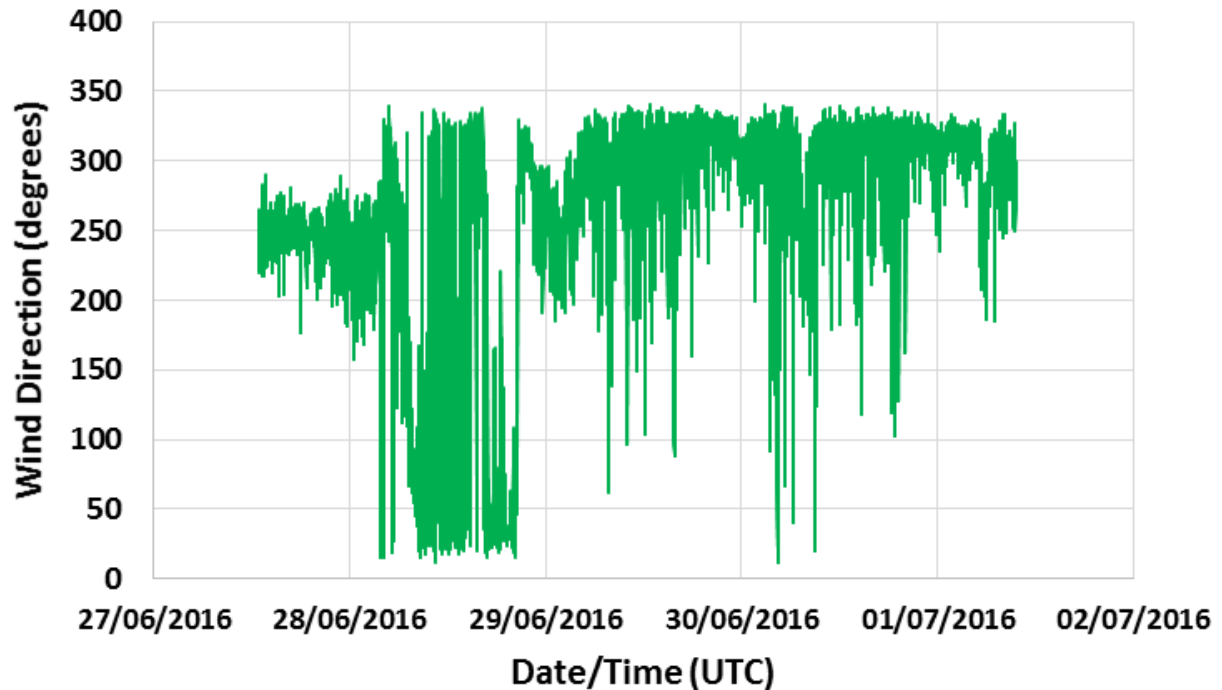


Figure 5.2: The wind direction plotted over the five-day period of the WST comparison (data provided by Southampton University).

## 6 CONCLUSIONS AND LESSONS LEARNT

The aim of this section is to highlight issues and lessons learnt during the 2016 WST radiometer comparison, so steps can be taken to avoid or diminish their effects in future comparisons. A number of participants have contributed to the contents of this section.

- i. The surface temperature of the target should be as spatially uniform as possible, at least in the region covered by the Field of View (FoV) of the participating radiometers. This is usually achieved under no wind and under calm water conditions. The wind speed and the condition of the surface of the water should be continuously monitored during the entire duration of future WST comparisons.
- ii. The area of the water observed by the different radiometers should be large enough to average out possible water surface temperature non-uniformities of the target.
- iii. Because different radiometers have different FoVs, it is recommended that in future WST comparisons, radiometers should be placed at different distances from the target being monitored so that the FoVs of the radiometers “cover” the same (identical) area of the water. The aim of this is to ensure that the same temperature non-uniformities on the surface of the water are seen (and averaged out) by every participating radiometer.
- iv. Care should be taken to ensure that all participating radiometers are observing the same area of the surface of the water.
- v. WST/SST measurements should ideally be performed in clear sky conditions. Failing that, measurements should be performed when the sky is completely covered



in cloud. Measurements performed under partly cloudy conditions should be avoided because of the difficulties in estimating the corrections due to the sky radiance which a partly cloudy condition introduces.

- vi. Ideally, each participant should either measure or obtain the emissivity of the sea/water from tables and use these emissivity values in calculating the surface temperature of the targets by taking into account the angle between the FoV of the radiometer and the surface of the water, as well as the wavelength band over which the radiometer has a finite response. However, it was recommended by some participants that in future comparisons, participants should be provided with a common emissivity estimate which could be used by the participants to calculate the WST of the targets.
- vii. When WST measurements are performed from platforms, care should be taken to prevent measurements being affected by possible blocking of surface water ripple by the structure of the platform on which the radiometers are mounted.
- viii. Care should be taken to prevent shadows of objects on the platform (on which the radiometers are mounted) from being in the radiometer viewing footprints. This can be achieved by mounting the radiometers on an extended arm so that they view footprints which are as far as possible away from the area affected by the shadows of the platform structure.
- ix. The effects of the shadows of the platform structure can be avoided/minimised by mounting the radiometers so that they face in a southern direction.

The 2016 WST comparison at Wraysbury reservoir allowed the full comparison of radiometers which are used for the validation of temperature measurements from radiometers operating on satellites. Measurements of the WST of the participating radiometers are within  $\pm 0.4$  °C of their arithmetic mean during the entire five-day duration of the comparison. However, the measurements of a radiometer which did not use a correction for the sky radiance was typically 0.6 °C from the mean, indicating the importance of using the sky radiance correction in sea surface temperature measurements.

## References

Barker Snook, I., Theocharous, E. and Fox, N. P., 2017, "2016 comparison of IR brightness temperature measurements in support of satellite validation. Part 2: Laboratory comparison of radiation thermometers", NPL Report ENV 14.

Barton, I. J., Minnett, P. J., Maillet K. A., Donlon, C. J., Hook, S. J., Jessup, A. T. and Nightingale, T.J., 2004, "The Miami 2001 infrared radiometer calibration and intercomparison: Part II Shipboard results", *Journal of Atmospheric and Oceanic Technology*, 21, 268-283.

Rice, J. P., Butler, J. I., Johnson, B. C., Minnett, P. J., Maillet K. A., Nightingale, T. J, Hook, S. J., Abtahi, A., Donlon, and. Barton, I. J., 2004, "The Miami 2001 infrared radiometer calibration and intercomparison. Part I: Laboratory characterisation of blackbody targets", *Journal of Atmospheric and Oceanic Technology*, 21, 258-267.

Theocharous, E., Fox, N. P., Sapritsky, V. I., Mekhontsev, S. N. and Morozova, S. P., 1998, “Absolute measurements of black-body emitted radiance”, *Metrologia*, **35**, 549-554.

Theocharous, E., Usadi, E. and Fox, N. P., 2010, “CEOS comparison of IR brightness temperature measurements in support of satellite validation. Part I: Laboratory and ocean surface temperature comparison of radiation thermometers”, NPL Report COM OP3.

Theocharous, E. and Fox, N. P., 2010, “CEOS comparison of IR brightness temperature measurements in support of satellite validation. Part II: Laboratory comparison of the brightness temperature of blackbodies”, NPL Report COM OP4.

Theocharous, E., Barker Snook, I. and Fox, N. P., 2017a, “2016 comparison of IR brightness temperature measurements in support of satellite validation. Part 1: Laboratory comparison of the brightness temperature of blackbodies”, NPL Report ENV 12.

Theocharous, E., Barker Snook, I. and Fox, N. P., 2017b, “2016 comparison of IR brightness temperature measurements in support of satellite validation. Part 4: Land surface temperature comparison of radiation thermometers”, NPL Report ENV 13.

## **Acknowledgements**

The authors wish to thank Mr Justin Ablitt, Mr Nick Lucas and Nick Crawford of NPL for their contributions to the measurement campaign at the open water test facility at Wraysbury reservoir. They also wish to thank Dr W. Wimmer of Southampton University for supplying the wind magnitude and direction data and for many useful discussions. They also wish to thank ESA for the financial support of this project. The University of Valencia participation in the 2016 FRM4STS comparison was funded by the Spanish Ministerio de Economía y Competitividad and the European Regional Development Fund (FEDER) through the project CGL2015-64268-R (MINECO/FEDER, UE) and by the Ministerio de Economía y Competitividad through the project CGL2013-46862-C2-1-P (MINECO).